VALIDATION OF NEAR INFRARED SPECTROSCOPY MEASUREMENTS OF SKELETAL MUSCLE OXIDATIVE CAPACITY

by

TERENCE EDWARD RYAN

(Under the Direction of Kevin K. McCully)

ABSTRACT

Skeletal muscle is one of the largest organs in the human body and its metabolic function is associated with both physical functioning and many pathologies. The mitochondrion is the main energy producing organelle in skeletal muscle cells, thus making its function vital for both health and disease. **Purpose:** The purpose of these studies was to validate a novel, non-invasive optical approach for assessing skeletal muscle (mitochondrial) oxidative capacity. **Methods:** Two experiments were performed. The first experiment utilized the well-known effects of endurance exercise, to induce a change in skeletal muscle oxidative capacity. Nine participants performed four weeks of forearm endurance exercise training, followed by five weeks of detraining. Skeletal muscle oxidative capacity was measured with near infrared spectroscopy (NIRS) every 5-7 days during both training and detraining. The seconds experiment was a cross validation between NIRS and the current gold standard *in vivo* approach, phosphorus magnetic resonance spectroscopy (^{31}P-MRS). Sixteen participants were tested with both NIRS and ^{31}P-MRS. **Results:** In the first study, the endurance exercise training resulted in a linear increase in oxidative capacity (NIRS rate constant) with a group average of 64

± 37% improvement after four weeks of exercise training ($p < 0.05$). Oxidative capacity declined exponentially upon cessation of exercise training, with a mean half-time of ~7.7 days. In the second study, the average recovery time constant was 31.5 ± 8.5 s for PCr and 31.5 ± 8.9 s for mVO_2 for all participants ($p = 0.709$). ^{31}P-MRS correlated well with NIRS for both Channel 1 (Pearson's $r = 0.88$, $p < 0.0001$) and Channel 2 (Pearson's $r = 0.95$, $p < 0.0001$). Furthermore, both ^{31}P-MRS and NIRS exhibit good repeatability between trials (CV = 8.1%, 6.9%, and 7.9% for NIRS Channel 1, NIRS Channel 2, and ^{31}P-MRS respectively). **Conclusion:** NIRS measurements of skeletal muscle oxidative capacity increased with endurance exercise training, decreased with detraining, and showed good agreement with ^{31}P-MRS. These findings support the validity of NIRS measurements of skeletal muscle oxidative capacity, and suggest that direct comparisons of NIRS and ^{31}P-MRS recovery rates can be made.

INDEX WORDS: NIRS, Mitochondrial Function, Oxidative Metabolism, Endurance Exercise

VALIDATION OF NEAR INFRARED SPECTROSCOPY MEASUREMENTS OF SKELETAL MUSCLE OXIDATIVE CAPACITY

by

TERENCE EDWARD RYAN

B.S., Florida State University, 2008

M.S., Florida Atlantic University, 2010

A Dissertation Submitted to the Graduate Faculty of The University of Georgia in Partial Fulfillment of the Requirements for the Degree

DOCTOR OF PHILOSPHY

ATHENS, GEORGIA

2013

VALIDATION OF NEAR INFRARED SPECTROSCOPY MEASUREMENTS OF SKELETAL MUSCLE OXIDATIVE CAPACITY

by

TERENCE EDWARD RYAN

Major Professor: Kevin McCully

Committee: Patrick O'Connor
Ellen Evans
Qun Zhao

Electronic Version Approved:

Maureen Grasso
Dean of the Graduate School
The University of Georgia
August 2013

DEDICATION

To Lauren for her never ending support, love, and sacrifices over the past few years. To my sister, Amy Ryan, you are on my mind each and every day. Your memory continues to push me forward. I would also like to dedicate this to my family for their continued support throughout my academic career. To our dog, Riley, for always letting me know when I have been reading or working too long each night!

ACKNOWLEDGEMENTS

I would like to thank the other members of the Exercise Vascular Biology Lab: Jared Brizendine, Melissa Erickson, Zoe Young, Michael Southern, Mary Ann Reynolds, and Sarah Stoddard. This work would not have been possible without the support and help of all of you. Our scientific discussions were always helpful and significantly contributed to the design of these studies. I also wish to thank Drs. Kevin McCully, Pat O'Connor, Ellen Evans, and Qun Zhao for serving on my committee and providing guidance throughout these studies, as well as during my time at UGA. Finally, I would like to thank all of the participants who volunteered for these studies. Without their generous commitment, this work would not have been possible.

TABLE OF CONTENTS

Page

ACKNOWLEDGEMENTS v

LIST OF TABLES viii

LIST OF FIGURES ix

CHAPTER

1 INTRODUCTION 1

Purposes 4

Hypotheses 4

Significance of the Study 5

2 REVIEW OF LITERATURE 6

Organization of Skeletal Muscle Energetics 6

Assessment of Skeletal Muscle Energetics 12

Mitochondria in Health and Disease 20

Summary 23

References 25

3 TRAINING- AND DETRAINING-INDUCED CHANGES IN SKELETAL MUSCLE METABOLISM WITH OPTICAL SPECTROSCOPY 43

Abstract 44

Introduction 45

Materials and Methods 47

Results....52
Discussion....53
References....59
4 VALIDATION OF NEAR INFRARED SPECTROSCOPY MEASUREMENTS OF SKELETAL MUSCLE OXIDATIVE CAPACITY WITH PHOSPHORUS MAGNETIC RESONANCE SPECTROSCOPY 71
Abstract....72
Introduction....73
Materials and Methods....74
Results....81
Discussion....84
References....89
5 SUMMARY AND CONCLUSIONS 104
References....111

LIST OF TABLES

Page

Table 2.1: Mitochondrial respiratory states 15

Table 3.1: Physical characteristics of the participants 65

Table 3.2: Weekly progression in training intensity 66

Table 3.3: Individual responses to exercise training and detraining.....67

Table 4.1: Physical characteristics of the participants 95

Table 4.2: Resting and end-exercise [PCr] and pH.....96

Table 4.3: NIRS and ^{31}P-MRS metabolic parameters 97

LIST OF FIGURES

Page

Figure 2.1: Graphical representation of the phosphocreatine shuttle 9

Figure 2.2: A typical ^{31}P-MRS measurement of mitochondrial function 18

Figure 2.3: A typical NIRS protocol.....19

Figure 2.4: Post-exercise recovery of mVO_2 measured with NIRS.....20

Figure 3.1: A representative testing protocol.....68

Figure 3.2: NIRS rate constants for the recovery of mVO_2 during exercise training and detraining 69

Figure 3.3: Percentage change in NIRS rate constant from baseline of the training arm..70

Figure 4.1: Recovery of phosphocreatine (PCr) and muscle oxygen consumption (mVO_2) after short duration plantarflexion exercise 98

Figure 4.2: Repeatability and reproducibility of ^{31}P-MRS and NIRS data.....99

Figure 4.3: Comparison between ^{31}P-MRS and NIRS data.....101

Figure 4.4: Signal-to-noise analysis of NIRS data.....102

Figure 4.5: Signal-to-noise analysis of ^{31}P-MRS data.....103

CHAPTER 1

INTRODUCTION

Skeletal muscle mitochondrial function is important for both health and sports performance. Mitochondria are the main energy producing organelles for cellular metabolism at rest, and during most exercise conditions. Impairments in mitochondrial function can result in decreased exercise tolerance and reduced quality of life (96). For example, skeletal muscle mitochondrial function is decreased in persons with multiple sclerosis (98), spinal cord injury (122), peripheral arterial disease (92), Friedreich's Ataxia (112, 113, 144), and diabetes (129). Chronic exercise training has been shown to enhance skeletal muscle mitochondrial function (6, 43, 50, 62, 117, 121, 151). John Holloszy coined the term mitochondrial biogenesis to describe the mitochondria's ability to change in response to stimuli. One of Holloszy's hallmark papers demonstrated the biochemical adaptations to muscle induced by exercise in rats in 1967 (90). In this study, rats performed 12 weeks of progressive treadmill exercise training. Mitochondrial oxygen uptake of the exercise-trained rats was twice the sedentary control rats. Similarly, succinate oxidase activity was approximately 50% greater in the exercising rats. Exercising rats also showed greater mitochondrial density, as inferred from concentrations of mitochondrial proteins.

Mitochondrial respiration can be directly measured using high-resolution respirometry. This technique requires a small sample of muscle tissue, called a muscle biopsy (19), and specialized equipment. Mitochondrial function and density have also

been inferred from concentrations of key enzymes such as citrate synthase (50) and succinate dehydrogenase (37) from muscle biopsies. A major disadvantage of these invasive techniques is that repeated measurements are too burdensome, especially for human subjects. Furthermore, biochemical assays of tissue samples are often stored prior to analysis, or even shipped off-site for analysis in a separate laboratory. These time delays could influence to outcome measurements.

With the development of magnetic resonance spectroscopy, non-invasive measurements of phosphate metabolites became possible. Kinetic changes in energy substrates like adenosine triphosphate (ATP), phosphocreatine (PCr), and inorganic phosphate (Pi) could be measured during muscle contractions and the recovery after muscle activity (4, 53, 124). Despite the advances in magnetic resonance technologies in the past 30 years, phosphorus magnetic resonance spectroscopy is still rarely used. The limited availability of multinuclear magnets and personnel with expertise in phosphorus spectroscopy has hindered its transition from research to clinical settings.

Near infrared spectroscopy (NIRS) uses low intensity light with wavelengths from 600 – 900 nm. The absorption characteristics of light in this range can provide information about the oxygenation status of heme (iron-containing) compounds. The main compounds with regard to muscle physiology are intravascular hemoglobin and intramyocellular myoglobin. Other compounds with similar molecular structures, such as cytochrome c and melanin, may also contribute to changes in the absorption/scattering characteristics (58, 74, 120). NIRS has been used to study muscle oxygenation (100), blood flow (131, 142), and muscle oxygen consumption (114, 142). Repeated measurements of muscle oxygen consumption (mVO_2) after exercise have been used to

measure the recovery of mVO_2 (130, 136). The rate of recovery of mVO_2 is directly proportional to the oxidative capacity of the muscle mitochondria. This technique was first proposed by Motobe and colleagues (130) and used to measure mitochondrial function in the forearm muscles of healthy young men. Changes in heme concentrations under the sampling area can influence NIRS signals (65), which are also visible in the data from Motobe et al. (130). Our lab has developed algorithms to correct NIRS signals for small changes heme concentration due to the passive redistribution of heme in the sampling tissue (136). With this technique, we have found good reproducibility between testing days (CV ~ 10%) in healthy young subjects. The NIRS rate of recovery of mVO_2 has been shown to be lower in patients with spinal cord injuries (54) compared with able-bodied controls. Similarly, the rate of recovery of mVO_2 from elite-level cyclists was nearly twice that of sedentary controls (22). The magnitude of difference in mitochondrial capacity measured in these two cross-sectional studies is similar to other techniques such as muscle biopsies (37, 43, 115) and magnetic resonance spectroscopy (117, 122, 123). Measuring the kinetic changes of mVO_2 with NIRS has significant advantages. Recovery rate calculations come directly from the exponential fits and are independent of the type and intensity of exercise or work performed. The rapid arterial occlusions necessary for these measurements require a continuous source of pressured air, but moderately large industrial compressors are inexpensive (~$500). Finally, NIRS devices themselves are inexpensive, widely available and do not require clearance for metal implants or claustrophobia.

Purposes

Considering the importance of mitochondrial function on health and disease, the goal of this research was to develop and validate a novel approach for measuring mitochondrial oxidative capacity using optical spectroscopy. Two experiments were performed. The purpose of the first study is to provide validation for NIRS measurements of mitochondrial capacity by measuring activity-induced changes in response to endurance exercise and detraining. Thirty days of endurance exercise training for the forearm flexors of the non-dominant arm will be performed thirty minutes per day, five days per week. NIRS measurements of mitochondrial capacity were performed bilaterally every 5-7 days during the training and for 30 days after the training. The purpose of the second study was to cross-validate the NIRS approach with the already well-established ^{31}P-MRS measure of phosphocreatine resynthesis. In the second study, direct comparisons were made between NIRS and ^{31}P-MRS recovery rates of mVO_2 and PCr respectively.

Hypotheses

The hypotheses for Study 1 are:

H_1) Endurance training of the forearm muscles will results in statistically significant increases in mitochondrial capacity measured with NIRS.

H_2) NIRS measured changes in mitochondrial capacity will be similar in magnitude to previous studies using other methods for measurement.

H_3) The time course of NIRS measured changes in mitochondrial capacity with training and detraining will be similar to literature values.

The hypotheses for study 2 are:

H_1) NIRS measurements of mitochondrial capacity will be significantly related (correlated) to MRS measurements of mitochondrial capacity.

H_2) The level of agreement between NIRS and MRS measurements will be strong (Pearson's $r > 0.5$).

H_3) Both NIRS and MRS measurements will be reproducible, consistent with literature values (Coefficient of variation of 10 – 20%).

Significance of the Study

Noninvasive methods for assessing skeletal muscle function can provide important insights to health and disease, as well as sports performance. NIRS devices are relatively inexpensive, and require little expertise for data collection. While the interpretation of NIRS data is more complicated, these devices hold promise for larger, multi-center clinical trials. Presently, the gold standard for noninvasive assessments of muscle metabolism rely on the use of multinuclear magnetic resonance facilities. These studies will provide essential information demonstrating the NIRS has the sensitivity to measure changes of mitochondrial capacity over time as well as a direct comparison of NIRS to the non-invasive gold standard, ^{31}P-MRS. The findings from these studies will help cement the validity of NIRS measurements of mitochondrial capacity, thus allowing for expansion of this technique to other researchers, physicians, and healthcare providers.

CHAPTER 2

REVIEW OF LITERATURE

Skeletal muscle is considered one of the largest organs in the human body and has the remarkable ability to rapidly alter its metabolism based on the imposed energy demand. Skeletal muscle metabolism consists of numerous enzymatic reactions and pathways, which may or may not rely on the availability of oxygen. Since skeletal muscle is the main contributor to energy expenditure, changes in skeletal muscle metabolism have been implicated in the pathogenesis of several diseases including aging, neurodegeneration, and diabetes (40, 92, 122, 141). Furthermore, skeletal muscle is considered a highly *plastic* tissue and retains the ability to change throughout the lifetime (90). This review of literature will describe the bioenergetic processes in skeletal muscle, and mechanisms for assessing skeletal muscle energetics including: in vitro high-resolution respirometry of isolated mitochondria, histochemical approaches with muscle biopsies, and non-invasive methods of phosphorus magnetic resonance spectroscopy and near-infrared spectroscopy. A discussion of the role of skeletal muscle metabolism in human health and disease as well as the effects of exercise interventions on changing muscle metabolism will also be presented.

Organization of Skeletal Muscle Energetics

Cells contain an enormous number of metabolic pathways that gives rise to the astounding complexity of bioenergetics. The study of skeletal muscle energetics is not a

new field. The earliest studies of muscle energetics involved the measurement of heat production during muscle contractions. Much of this work was pioneered by English physiologist, A.V. Hill (2, 55, 76, 83, 85-89); although Hill cites the earlier studies performed by Hermann von Helmholtz in 1848 on the mechanical foundations of muscle thermodynamics (99).

Adenosine triphosphate (ATP) is considered the major unit of currency for cellular energetics. The chemical breakdown of ATP provides the free energy necessary for normal cellular maintenance as well as the extreme energetic demands of skeletal muscle contraction (23, 24, 44). Humans produce ATP through the biochemical breakdown of macronutrients such as carbohydrates, fats, and proteins. In spite of the profound complexity of cellular energetics, below is a simplified description of the main energy systems involved in the production of ATP in skeletal muscle cells.

ATP-consuming reactions during skeletal muscle contractile activity can be largely attributed to two factors: myosin and sarco-endoplasmic reticulum ATPase's (SERCA), and the contraction type (i.e. concentric, eccentric, isometric). From an ATPase standpoint, the myosin ATPase is responsible for approximately 60% of the ATP consumption during skeletal muscle contraction, while the SERCA accounts for ~30% (139). Furthermore, the different isoforms of these enzymes influence the ATP cost of contractile activity (134). For example, Harkema et al. (75) estimated the ATP cost of brief tetanic contractions, from direct measures of PCr change, to be threefold higher in the biceps brachii (fast-twitch) compared with soleus (slow-twitch) cat muscles. Crow and Kushmerick (41) reported similar results for slow (soleus) and fast (extensor digitorum longus) murine muscles nearly fifteen years early.

The mechanical nature and force of the muscle contraction also plays and important role in determining the ATP cost of contraction. Contractile ATP use increases linearly with the time tension integral (i.e. force x time-under-tension) (125). Moreover, the ATP cost is dependent on the type of contraction. The earliest reports suggesting differential energy cost for contraction types came from American physiologist, Wallace Fenn in 1923 (56, 57). In these experiments, Fenn found that shortening contractions of isolated frog sartorius muscle 'liberated more energy' compared to isometric contractions. More recently, He et al. (79) reported that ATP consumption rates increased in proportion to shortening velocity using in vitro permeabilized human muscle fibers. Similarly, in vivo measurements of PCr consumption (as a direct indicator of ATP cost) were greater in concentric muscle contractions compared with isometric and eccentric (137).

ATP-phosphocreatine energy system represents an immediate supply of energy stored within muscle cells (23, 24). Skeletal muscle cells contain relatively low concentrations of ATP (~5.5 mM/kg wet weight or ~8.2 mM). This stored ATP serves as an immediate source of energy for cellular activity (Equation 2.1). Phosphocreatine (PCr) is stored in muscle cells at nearly five times the concentration of ATP (approximately 30 mM). PCr is analogous to a chemical pH buffer in that it serves as a source to directly rephosphorylate ADP. The reaction is catalyzed by the enzyme creatine kinase (CK) and the overall reaction can be seen below:

$$MgATP^{2-} \xrightarrow{ATPase} MgADP^{-} + P_i + H^{+} \quad \text{(Equation 2.1)}$$

$$MgADP^{-} + PCr^{2-} + H^{+} \overset{CK}{\leftrightarrow} MgATP^{2-} + Cr \quad \text{(Equation 2.2)}$$

This reaction serves to buffer changes in the phosphorylation potential (i.e. [ATP]/[ADP]). The ATP/ADP ratio remains relatively high, even during intense exercise. Thus, large changes in the PCr/Cr ratio buffer small changes in ATP/ADP. To better understand this CK system, two concepts must be explained: (1) the CK enzyme is extremely active, and thus considered to be at equilibrium in most conditions; (2) the many isoforms of CK (i.e. cytosolic and mitochondrial) give rise to a transport system known as the "phosphocreatine shuttle" (20, 126). This transport system serves to continuously supply PCr to the myofibrils (or cytosol) through rephosphorylation of Cr in the mitochondria, thus ensuring muscle contractile activity can continue (Figure 2.1).

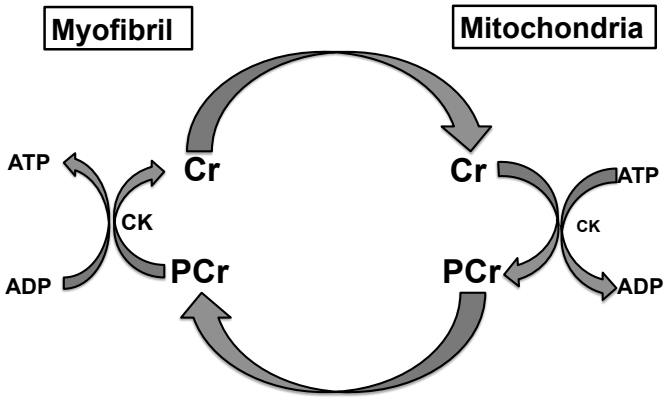

Figure 2.1. Graphical representation of the phosphocreatine shuttle.

While the above reactions are those studied in human muscle energetics, other reactions that may be of importance under certain circumstances include the adenylate kinase reaction, which catalyzes the production of ATP and AMP from two ADP molecules. Furthermore, AMP accumulation is rarely found in physiological conditions due to its rapid deamination to inosine monophosphate.

The Glycolytic energy system has a greater capacity for generating ATP compared with the ATP-PCr system due to greater concentrations of stored glycogen. However, glycolysis alone, without oxidative phosphorylation, only has the capacity to support skeletal muscle contractions for less than one minute. The glycolytic pathway was originally described by German biochemist Otto Meyerhof (127). This glycolytic pathway consists of nine or ten enzyme-catalyzed reactions, depending on the starting substrate (glucose versus glycogen). The general glycolytic reactions for the breakdown of glucose and glycogen are below in Equations 2.3 and 2.4.

$$Glucose + 2ADP + 2P_i + 2NAD^+ \rightarrow 2Pyruvate + 2ATP + 2NADH + 2H^+ \quad \text{(Equation 2.3)}$$

$$Glycogen_n + 3ADP + 3P_i + 2NAD^+ \rightarrow Glycogen_{n-1} + 2Pyruvate + 3ATP + 2NADH + H^+ \quad \text{(Equation 2.4)}$$

Glycogen metabolism produces an additional ATP due to its entry into glycolysis, which skips the energy consuming reaction catalyzed by the enzyme hexokinase. From the above two reactions, one can conclude that glycolytic metabolism has two main functions: (1) the productions of ATP for cellular energy, and (2) production of pyruvate and the reduction of NAD to $NADH^+$ both of which can be further metabolized in the mitochondria. Under hypoxic conditions, pyruvate can be further broken down into lactate by the enzyme lactate dehydrogenase, in order to continue supplying the NAD required for glycolytic ATP production. The anaerobic production of lactate is metabolically inefficient as most of the molecular energy remains in this three-carbon sugar. In contrast, when oxygen is present, the pyruvate can be further metabolized in the mitochondria to produce additional ATP via oxidative phosphorylation.

Oxidative phosphorylation is a term that collectively describes the net oxidation of nutrients to produce ATP in the mitochondria. Two main pathways that make up oxidative phosphorylation include the Krebs cycle (or Citric acid cycle, or tricarboxylic acid cycle) and the electron transport system (ETS). The Krebs cycle (101-106) is a metabolic pathway that takes place in the matrix of the mitochondria, which involves the transfer of electrons from acetyl groups to nicotinamide adenine dinucleotide (NAD) and flavin adenine dinucleotide (FAD). These two reduced electron carriers can then be transferred to the ETS for oxidation. The ETS consists of several multi-polypeptide protein complexes embedded in the inner mitochondrial membrane that receive electrons for the soluble matrix dehydrogenases (NAD and FAD). These electrons are transferred through a series of electron carriers in the respiratory chain ordered in such a way that their redox potentials progressively decrease from NADH (Complex I) to O_2 (terminal electron acceptor). In three of the ETS protein complexes (I, III, and IV), the fall in redox potential across the oxidation-reduction reactions within each complex is sufficient to drive the translocation of protons from the matrix to the inner membrane space. This creates a proton gradient across the inner membrane that is composed of both the concentration difference (ΔpH) and the electrical potential ($\Delta\tilde{u}_H^+$), which together are commonly referred to as the membrane potential ($\Delta\Psi$). This membrane potential is the essence of Peter Mitchell's chemiosmotic theory (which he was awarded the Nobel Prize in Chemistry in 1978) whereby the accumulation of $\Delta\Psi$ is sufficient to the drive the synthesis of ATP as protons flow back through the ATP synthase complex (F_1F_0 Complex) into the matrix (128). The net reactions for oxidative phosphorylation of

pyruvate and a sixteen-carbon fatty acid are found below in Equations 2.5 and 2.6 respectively.

$$2C_3H_6O_3 + 6O_2 + 2NADH + 33ADP + 33P_i \rightarrow 6CO_2 + 6H_2O + 2NAD + 33\ ATP \quad \text{(Equation 2.5)}$$

$$C_{16}H_{32}O_2 + 23O_2 + 129\ ADP + 129P_i \rightarrow 16CO_2 + 16H_2O + 129\ ATP \quad \text{(Equation 2.6)}$$

Clearly, the mitochondrial oxidative phosphorylation is the only metabolic source with the capacity to generate ATP for sustained muscle contractile activity.

An important concept that is commonly misconstrued in basic exercise physiology texts is that the control of these pathways is depicted as a hierarchy. For example, at the onset of exercise, the initial ATP is supplied by the ATP-PCr energy system. If exercise continues, the short-term or glycolytic energy system is turned on the produce ATP for exercises with a longer duration (~2 minutes). If exercise if prolonged, the aerobic energy system, or mitochondrial oxidative phosphorylation, is turned on to produce the energy required. In actuality, these pathways respond immediately and simultaneously in response to the breakdown of ATP and release of calcium. In fact, the activation of mitochondrial oxidative phosphorylation has been reported to be on the order of seconds (31), with ADP being the primary stimulant.

Assessment of Skeletal Muscle Energetics

Numerous techniques have been used in the study of muscle energetics. Early work from A.V. Hill and colleagues measured heat production from isolated frog muscles during muscle contractions as an indication of muscle energetics (1, 2, 55, 76, 81-86, 88, 89). With the advancement of technology, it became possible to make accurate

biochemical assessments using respirometry, optical spectroscopy, histochemistry, and magnetic resonance spectroscopy.

In vitro respirometry has a storied history that began with the works of British physiologists, John Haldane (67-73) and Joseph Barcroft (7-16, 18). Haldane's first apparatus pumped out oxygen released from blood into a gas buret for measurement (69). However, Haldane's first device made measurements tedious, so later Barcroft and Haldane built blood-gas analyzers that exploited the arterial-venous oxygen difference as an indication of tissue respiration (12). Barcroft's apparatus was later improved by the addition of an oil solution, which improved calculations of blood oxygenation (17). Unfortunately for Barcroft, his apparatus later became known as the Warburg apparatus, after German physiologist Otto Warburg. Warburg used Barcroft's apparatus to assess tumor cell respiration among other things (146-149). This same device is the basis for many of the modern respirometers, which remains largely unchanged.

Modern-day respirometry equipment is typically used in cellular and molecular biology labs, mostly by basic scientists interested in studying mitochondrial bioenergetics. These techniques require isolation of mitochondria from mammalian muscle samples, with a relatively large amount of mitochondrial tissue required for respiration measurements (50-70 mg) (63, 64). The isolated mitochondria are placed into a medium-filled chamber that allows for the addition of substrates (ADP, glutamate, malate) and oxygen. This technique has significantly advanced over the past ~15 years, by using a modified approach with permeabilized myofibers. Using a plant-based detergent, saponin, which extracts cholesterol from the sarcolemma and thus perforates the membrane, allowing substrates to freely exchange with the preparation medium.

Intracellular membrane-bound organelles such as mitochondria contain very low concentrations of cholesterol, thus the structural integrity of the mitochondrial reticulum is retained. This approach also allows for respirometric measurements with very small sampled of muscle tissue (~0.1 mg). The major advantage of respirometry is that precise measures of oxygen consumption and ATP production can be made with these devices, using standardized titration protocols that maintain appropriate oxygen concentrations while controlling the addition of energetic substrates. For example, in 2011, Larsen et al. (108) demonstrated and improved mitochondrial P/O ratio (and indication of efficiency) in isolated human skeletal muscle mitochondria following nitrate supplementation. In vitro respirometry has the ability assess respiratory capacity at multiple levels of the respiratory chain. Anderson and colleagues (3) recently demonstrated that obese males exhibited decreased State 3 respiration (maximal ADP-stimulated oxygen consumption by mitochondria) and increased production of H_2O_2 (a byproduct of reactive oxygen species) compared with lean men. Similarly, Mogensen et al. also used high-resolution respirometry to show that Type II diabetics had lower State 3 respiration compared with non-diabetic controls (129).

Britton Chance's development of the dual wavelength spectrophotometer (25) led to a pivotal group of papers that outline mitochondrial respiration (27, 31-34, 36). Using this optical spectrometer, Chance and colleagues reported the kinetics of mitochondrial respiration and showed that ADP is the major stimulus for increasing respiration (35).

Below in Table 2.1 is a summary of Chance's mitochondrial respiratory states.

Table 2.1. Mitochondrial respiratory states.

State	$[O_2]$	ADP level	Substrate level	Respiration rate	Rate-limiting substance	Description
1	>0	Low	Low	Slow	ADP	Mitochondria alone
2	>0	High	~0	Slow	Substrate	Substrate added, low ADP
3	>0	High	High	Fast	Respiratory chain	Limited amount of ADP added
4	>0	Low	High	Slow	ADP	All ADP converted to ATP
5	<0	High	High	0	Oxygen	Anoxia

Histochemical approaches have also been used make inferences about mitochondrial function. Using the muscle biopsy technique (19), a sample of muscle tissue is obtained for histochemical assays. Increases in protein content of vital mitochondrial enzymes such as citrate synthase (CS) and succinate dehydrogenase (SDH) have been commonly used as markers of both mitochondrial function and density (6, 52). While mitochondrial density is more accurately determined using electron microscopy, protein content changes have been shown to parallel those found with electron microscopy (135).

In 1967, John Holloszy found that rats subjected to treadmill running had two-fold increase in the mitochondrial respiratory capacity was accompanied by 60% increase in mitochondrial protein content (90). In further support of oxidative enzyme levels being related to mitochondrial function, Chi et al. (37) showed that levels of CS and SDH decreased after 12 weeks of detraining. Recent advances in molecular biology, has allowed researchers to measure intracellular signaling molecules linked with

mitochondrial adaptation as well as levels of messenger RNA associated with mitochondrial biogenesis.

Phosphorus magnetic resonance spectroscopy (^{31}P-MRS) exploits the biophysical characteristics of nuclear spins exposed to strong magnetic fields. Several well-known scientists can be credited with the development and implementation of ^{31}P-MRS for studying skeletal muscle including Britton Chance, George Radda, Rex Richards, Jack Leigh, and others. Some of the earliest ^{31}P-MRS studies on muscle tissue were published in the late 1970's by Joan Dawson (45, 46). Since its inception, ^{31}P-MRS has been extensively used to study skeletal muscle energetics and is becoming increasingly popular as the number of multi-nuclear magnetic resonance imagers grows.

In order to explain the ^{31}P-MRS, a brief review of the basic principles is necessary. Nuclear magnetic resonance (NMR) is based on the concept of nuclear spin. Atoms with an odd number of protons and/or neutrons possess a nuclear spin angular momentum, and therefore are useful to NMR. Examples of these nuclei with biological importance include hydrogen (^{1}H), phosphorus (^{31}P), carbon (^{13}C), sodium (^{23}Na), and fluorine (^{19}F). In the presence of a strong, external magnetic field, the magnetic moments of these nuclei tend to align with the external magnetic field. These nuclei also precess at given frequency (called the Larmor Frequency) that is a function of the nuclei's chemical environment, as well as the strength of the external magnetic field. To obtain an NMR signal, a radiofrequency pulse tuned to the resonant frequency is applied in the transverse plane to excite the nuclear spins out of equilibrium. The excited, rotating nuclei induce an electromotive force in the MR coil, which decays over time as the nuclei give off energy to the surround environment.

^{31}P-MRS has been used to measure changes in phosphorus metabolites of skeletal muscle including: phosphocreatine (PCr), inorganic phosphate (Pi), and adenosine triphosphate (ATP). Other metabolites such ADP, sugar phosphate (glycerol-6-phophate), NADPH can be seen in extreme conditions, but in most physiological circumstances the concentrations are too low for detection with ^{31}P-MRS. Early studies in skeletal muscle energetics examined changes in metabolite concentration to various steady-state exercise levels, using the data to extrapolate a maximal mitochondrial oxidative capacity using a Michaelis-Menton enzyme kinetics approach (29, 30). As NMR technologies continued to advance, the quality of equipment and data resulted in the ability to collect quality phosphorus spectra at higher time resolution (using less signal averaging). The allowed the study of kinetic changes in metabolites during exercise and the recovery from exercise (124). The kinetics for the resynthesis of PCr after exercise has been largely considered the gold standard for in vivo measurement of mitochondrial oxidative capacity and have been utilized extensively in the past ~25 years (21, 28, 39, 60, 61, 77, 78, 91, 92, 96, 97, 109, 110, 116, 118, 119, 121, 123, 124, 132, 145). Figure 2.2 shows a typical ^{31}P-MRS measurement of the recovery of phosphocreatine after short duration plantar flexion exercise.

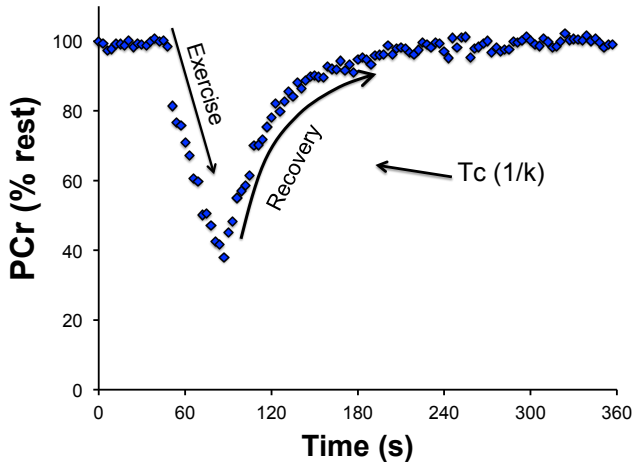

Figure 2.2. A typical ^{31}P-MRS measurement of mitochondrial function. Each triangle represents a single measurement of the concentration of phosphocreatine (PCr). Short duration exercise is used to deplete PCr, and the subsequent recovery post-exercise. The time constant (Tc) is inversely related to mitochondrial function; while the rate constant (k = 1/Tc) is directly proportional to mitochondrial function.

Near-infrared spectroscopy is a non-invasive, optical technique that uses near infrared light to estimate brain, blood, and tissue oxygenation. Light in the near infrared region [wavelength (λ) = 600 – 900 nm] can easily penetrate biological tissues (93). Several chromophores in skeletal muscle have the ability to absorb NIR light, but the two main chromophores are hemoglobin (Hb) and myoglobin (Mb). Furthermore, the absorption and scattering characteristics of Hb and Mb are dependent on whether they are bound to oxygen. Therefore NIRS can be used to measure skeletal muscle oxygenation (26), blood flow (49, 59), and oxygen consumption (47, 138, 142, 143). Recently, Motobe and colleagues suggested that repeated measurements of muscle oxygen consumption during the recovery from exercise could provide an index of mitochondrial capacity (130). Our lab has modified this approach to improve the accuracy and reliability of NIRS data by correcting NIRS signals for changes in blood volume (136).

Figure 2.3 shows a typical NIRS protocol where arterial occlusions were made at rest to measure resting oxygen consumption, followed by two exercise/recovery trials.

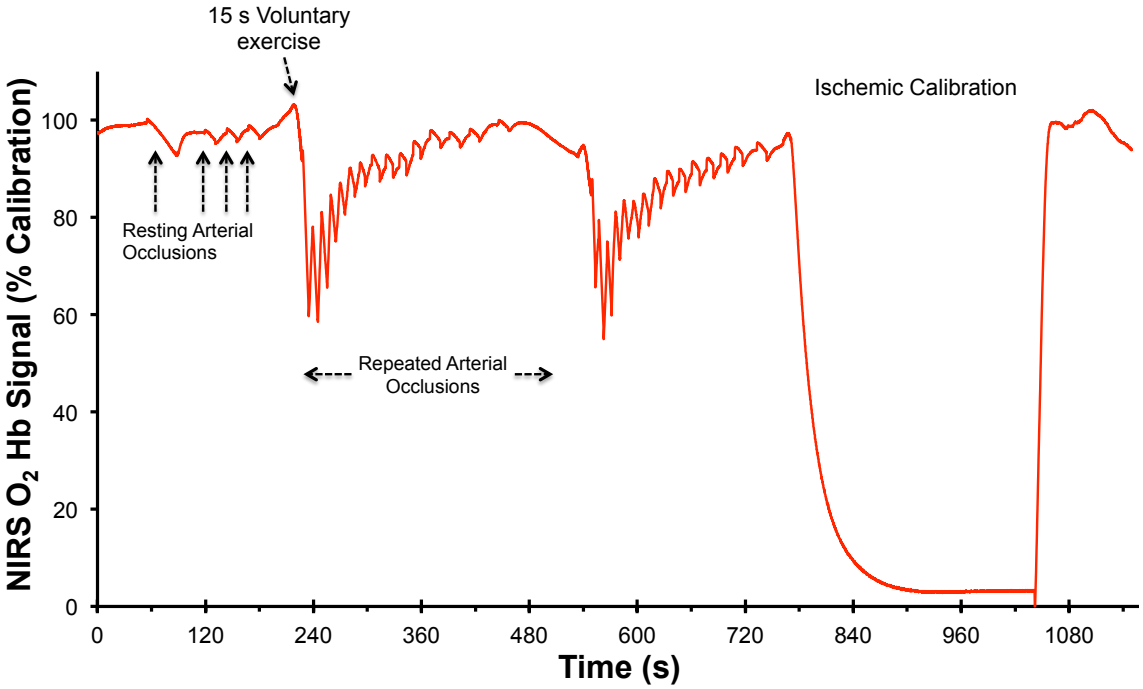

Figure 2.3. A typical NIRS protocol showing measurements of resting oxygen consumption, mitochondrial function, and an ischemic calibration procedure.

For each exercise/recovery trial, short duration exercise is performed to increase skeletal muscle oxygen consumption. After cessation of exercise, a series of short, repeated arterial occlusions are performed, each providing a measurement of oxygen consumption. The protocol ends with an ischemic calibration procedure, which consists of a 3 – 6 minute arterial occlusion (to deplete all oxygen levels, providing a "zero" oxygen level) followed by a hyperemic response upon release of the cuff (indicating 100% oxygen).

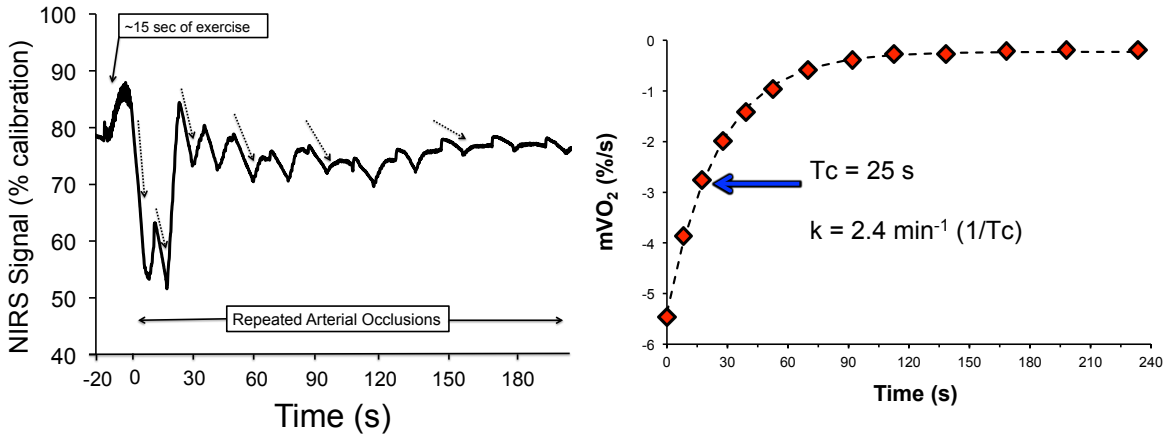

Figure 2.4. Post-exercise recovery of muscle oxygen consumption (mVO_2) measured with NIRS. The slope of the NIRS signal during each arterial occlusion provides a measure of mVO_2. The recovery kinetics of mVO_2 following exercise are well characterized by a mono-exponential function.

Figure 2.4 shows post-exercise measurements of oxygen consumption, and the recovery kinetics of muscle oxygen consumption after exercise.

Some advantages of NIRS devices include the relatively low cost, ease of data collection, and the availability and portability of these devices. NIRS also has several limitations. For example, NIRS measurements of mitochondrial capacity are limited only to peripheral limb muscles. Accurate quantification of NIRS signals is also a major limitation. To quantify NIRS signals, information about the absorption and scattering characteristics and the concentrations of Hb and Mb (and their relative contributions to the overall NIRS signal) is required. Currently, NIRS the most commonly used NIRS devices (continuous-wave NIR light) cannot provide this information, and thus measure relative changes in the level of oxygenation.

Mitochondria in Health and Disease

The modern day mitochondrion is an evolved form of protobacterium which symbiosed a eukaryotic cell nearly 1.5 billion years ago (5, 66). Mitochondria have

several functions including cellular signaling, differentiation, growth, and death; but are most known for their role as key regulators of metabolism within the cell by converting energy from the oxidation of macronutrients to adenosine triphosphate (ATP). Since skeletal muscle is the main contributor to energy expenditure, changes skeletal muscle mitochondrial function have been implicated in the pathogenesis of several diseases such as aging, neurodegeneration, and Type 2 diabetes (40, 92, 122, 141). Skeletal muscle mitochondria have a remarkable ability to alter the genotype and phenotype in response to changes in demand, which has been commonly termed *mitochondrial plasticity*. The first convincing demonstration of mitochondrial plasticity was provided by John Holloszy (90), who showed that both the mitochondrial enzyme content and isolated mitochondrial oxygen uptake increased with endurance exercise in rat muscle. In the time since Holloszy's experiments, more than 3000 articles have been published, enhancing our understanding of mitochondrial adaptations to exercise as well as disease or disuse. The general term used to describe these molecular mechanisms is mitochondrial biogenesis. In contrast, a lack of physical activity and/or disease lead to a chronic state of low energy demand which results in a loss of mitochondrial volume and decreased respiratory capacity (94).

Control of mitochondrial biogenesis involves the coordinated response of signaling pathways and factors from both nuclear and mitochondrial genomes. Mitochondrial biogenesis can be induced by numerous physiological, environmental, and pharmacological stimuli and results in the transcription and translation of nuclear and mitochondrial genes. Skeletal muscle contractile activity induces adaptations that are dependent upon the type of exercise (i.e. resistance vs. endurance), as well as the training

characteristics such as intensity, frequency and duration (51). Contractile activity initiates signaling pathways through activated transcription factors: AMP kinase (AMPK), Ca^{2+}-calmodulin-activated protein kinase (CaMK), nuclear respiratory factors (NRF-1 and NRF-2), and peroxisome proliferator-activated proteins (PPAR-α and PPAR-γ); which are activated through calcium and AMP signal transduction pathways. Moreover, NRF-1 and NRF-2 are responsible for the link between mitochondrial and nuclear genomes, through their activation of mitochondrial transcription factor A (TFAM). However, the binding of transcription factors to gene promotors alone is not sufficient to activate genes transcription. This often requires the enzymatic activity of coactivator proteins, such as peroxisome proliferator coactivator (PGC-1α) to stimulate the expression of both nuclear and mitochondrial genes. Activation of PGC-1α occurs through phosphorylating reactions by two protein kinases: p38 mitogen activated protein kinase (p38 MAPK) and AMPK. Endurance exercise initiates mitochondrial biogenesis through PGC-1α in both acute and chronic conditions. Acute and chronic bouts of endurance exercise result in an increase in phosphorylated PGC-1α and the translocation of PGC-1α from the cytosol to the nucleus (133, 150), which initiates the above intracellular signaling cascade ultimately resulting in mitochondrial proliferation and increased function of existing mitochondria.

In contrast, several mitochondrial changes are also associated with physical inactivity, aging, and chronic disease. For example, aging is associated with a reduction in mitochondrial content and oxidative capacity (80, 107). A chronic lack of physical activity also results in a significant decrease in the mitochondrial function. Paralysis, secondary to a traumatic spinal cord injury, represents one of the most dramatic models

of inactivity available in human studies. Mitochondrial oxidative capacity in paralyzed musculature is approximately one-half to one-third that of a sedentary, non-paralyzed muscle (111, 115, 122, 140). Reduced mitochondrial function has also been reported in other neuromuscular conditions such as Friedreich's Ataxia (144) and multiple sclerosis (98). Mitochondrial dysregulation has also been implicated in the pathogenesis of metabolic diseases such as diabetes and insulin resistance (95). A reduced mitochondrial oxidative capacity has been reported in diabetic muscle in some studies (42, 141) but not others (48). The underlying discrepancy between these studies is a lack of control in the physical activity levels of the participants. Regular exercise might protect the mitochondria from a decrease in oxidative capacity. Thus reduced mitochondrial capacity may well be a consequence of diabetes rather than a cause. Skeletal muscle mitochondrial energetics have also been linked to functional capacity. Coen et al. reported that mitochondrial oxidative capacity was associated with maximal whole-body aerobic capacity and walking speed in older adults (38).

Summary

Mitochondria are commonly referred to as the "powerhouse" of the cell, because of their role in producing the cellular energy currency ATP. Properly functioning mitochondrial are, therefore, vital in maintain cellular homeostasis, especially in the demands of increased ATP breakdown cause by muscular contraction. Thus, alterations in mitochondrial capacity will have tremendous impact on the functional capacity of the organism. Measurements of mitochondrial oxidative capacity have been made for more than 100 years. Traditionally, in vitro techniques have been used, but these require isolation of skeletal muscle tissue. The development of non-invasive methodologies for

study mitochondrial capacity will greatly enhance the ability of researchers and clinicians to make measurements on human participants, especially those with chronic diseases. Information gained from studying mitochondrial capacity in various populations will help guide therapeutic and pharmacological interventions aimed to improve the overall health and functional capacity of humans.

References

1. Abbott BC, Downing AC, and Hill AV. Rapid equipment for recording muscle heat. *J Physiol* 106: 31, 1947.

2. Abbott BC, and Hill AV. The heat of shortening of muscle. *J Physiol* 109: Proc, 7, 1949.

3. Anderson EJ, Lustig ME, Boyle KE, Woodlief TL, Kane DA, Lin CT, Price JW, 3rd, Kang L, Rabinovitch PS, Szeto HH, Houmard JA, Cortright RN, Wasserman DH, and Neufer PD. Mitochondrial H2O2 emission and cellular redox state link excess fat intake to insulin resistance in both rodents and humans. *The Journal of clinical investigation* 119: 573-581, 2009.

4. Arnold DL, Matthews PM, and Radda GK. Metabolic Recovery after Exercise and the Assessment of Mitochondrial-Function Invivo in Human Skeletal-Muscle by Means of P-31 Nmr. *Magn Reson Med* 1: 307-315, 1984.

5. Balaban RS, Nemoto S, and Finkel T. Mitochondria, oxidants, and aging. *Cell* 120: 483-495, 2005.

6. Baldwin KM, Cheadle WG, Martinez OM, and Cooke DA. Effect of functional overload on enzyme levels in different types of skeletal muscle. *Journal of applied physiology: respiratory, environmental and exercise physiology* 42: 312-317, 1977.

7. Barcroft J. Differential method of blood-gas analysis. *The Journal of physiology* 37: 12-24, 1908.

8. Barcroft J. The gaseous metabolism of the kidney. *The Journal of physiology* 32: 18-27, 1904.

9. Barcroft J. The gaseous metabolism of the submaxillary gland. *The Journal of physiology* 27: 31-47, 1901.

10. Barcroft J. The gaseous metabolism of the submaxillary gland: Part I. On methods, with a description of an apparatus for gas analysis. *The Journal of physiology* 25: 265-282, 1900.

11. Barcroft J. The gaseous metabolism of the submaxillary gland: Part II. On the absorption of water from the blood during its passage through the active gland. *The Journal of physiology* 25: 479-486, 1900.

12. Barcroft J. A method of estimating the oxygen and carbonic acid in small quantities of blood. *The Journal of physiology* 28: 232-240, 1902.

13. Barcroft J, and Brodie TG. The gaseous metabolism of the kidney. *The Journal of physiology* 33: 52-68, 1905.

14. Barcroft J, and Dixon WE. The gaseous metabolism of the mammalian heart: Part I. *The Journal of physiology* 35: 182-204, 1907.

15. Barcroft J, and Higgins HL. The determination of the constants of the differential blood-gas apparatus. *The Journal of physiology* 42: 512-518, 1911.

16. Barcroft J, and Piper H. The gaseous metabolism of the submaxillary gland with reference especially to the effect of adrenalin and the time relation of the stimulus to the oxidation process. *The Journal of physiology* 44: 359-373, 1912.

17. Barcroft J, and Roberts F. Improvements in the technique of blood-gas analysis. *The Journal of physiology* 39: 429-437, 1910.

18. Barcroft J, and Shore LE. The gaseous metabolism of the liver: Part I. In fasting and late digestion. *The Journal of physiology* 45: 296-306, 1912.

19. Bergstrom J. Muscle-biopsy needles. *Lancet* 1: 153, 1979.

20. Bessman SP, and Geiger PJ. Transport of energy in muscle: the phosphorylcreatine shuttle. *Science* 211: 448-452, 1981.

21. Blei ML, Conley KE, Odderson IR, Esselman PC, and Kushmerick MJ. Individual Variation in Contractile Cost and Recovery in a Human Skeletal-Muscle. *P Natl Acad Sci USA* 90: 7396-7400, 1993.

22. Brizendine JT, Ryan TE, Larson RD, and McCully KK. Skeletal muscle metabolism in endurance athletes with near infrared spectroscopy. *Med Sci Sports Exerc* 45(5):869-875, 2013.

23. Cain DF, and Davies RE. Breakdown of adenosine triphosphate during a single contraction of working muscle. *Biochem Biophys Res Commun* 8: 361-366, 1962.

24. Cain DF, Infante AA, and Davies RE. Chemistry of muscle contraction. Adenosine triphosphate and phosphorylcreatine as energy supplies for single contractions of working muscle. *Nature* 196: 214-217, 1962.

25. Chance B. Rapid and sensitive spectrophotometry. III. A double beam apparatus. *Rev Sci Instru* 22: 634-638, 1951.

26. Chance B, Dait MT, Zhang C, Hamaoka T, and Hagerman F. Recovery from exercise-induced desaturation in the quadriceps muscles of elite competitive rowers. *The American Journal Of Physiology* 262: C766-775, 1992.

27. Chance B, Eleff S, Leigh JS, Jr., Sokolow D, and Sapega A. Mitochondrial regulation of phosphocreatine/inorganic phosphate ratios in exercising human muscle: a gated 31P NMR study. *P Natl Acad Sci USA* 78: 6714-6718, 1981.

28. Chance B, Im J, Nioka S, and Kushmerick M. Skeletal muscle energetics with PNMR: personal views and historic perspectives. *NMR In Biomedicine* 19: 904-926, 2006.

29. Chance B, Leigh JS, Clark BJ, Maris J, Kent J, Nioka S, and Smith D. Control of Oxidative-Metabolism and Oxygen Delivery in Human Skeletal-Muscle - a Steady-State Analysis of the Work Energy-Cost Transfer-Function. *P Natl Acad Sci USA* 82: 8384-8388, 1985.

30. Chance B, Leigh JS, Smith DS, Nioka S, and Clark BJ. Phosphorus Magnetic Resonance Spectroscopy Studies of the Role of Mitochondria in the Disease Processa. *Annals of the New York Academy of Sciences* 488: 140-153, 1986.

31. Chance B, and Williams GR. Respiratory enzymes in oxidative phosphorylation. I. Kinetics of oxygen utilization. *The Journal of biological chemistry* 217: 383-393, 1955.

32. Chance B, and Williams GR. Respiratory enzymes in oxidative phosphorylation. II. Difference spectra. *The Journal of biological chemistry* 217: 395-407, 1955.

33. Chance B, and Williams GR. Respiratory enzymes in oxidative phosphorylation. III. The steady state. *The Journal of biological chemistry* 217: 409-427, 1955.

34. Chance B, and Williams GR. Respiratory enzymes in oxidative phosphorylation. IV. The respiratory chain. *The Journal of biological chemistry* 217: 429-438, 1955.

35. Chance B, and Williams GR. Respiratory enzymes in oxidative phosphorylation. VI. The effects of adenosine diphosphate on azide-treated mitochondria. *The Journal of biological chemistry* 221: 477-489, 1956.

36. Chance B, Williams GR, Holmes WF, and Higgins J. Respiratory enzymes in oxidative phosphorylation. V. A mechanism for oxidative phosphorylation. *The Journal of biological chemistry* 217: 439-451, 1955.

37. Chi MM, Hintz CS, Coyle EF, Martin WH, 3rd, Ivy JL, Nemeth PM, Holloszy JO, and Lowry OH. Effects of detraining on enzymes of energy metabolism in individual human muscle fibers. *The American Journal Of Physiology* 244: C276-287, 1983.

38. Coen PM, Jubrias SA, Distefano G, Amati F, Mackey DC, Glynn NW, Manini TM, Wohlgemuth SE, Leeuwenburgh C, Cummings SR, Newman AB, Ferrucci L, Toledo FG, Shankland E, Conley KE, and Goodpaster BH. Skeletal Muscle Mitochondrial Energetics Are Associated With Maximal Aerobic Capacity and Walking Speed in Older Adults. *J Gerontol A Biol Sci Med Sci* 2012.

39. Conley KE, Jubrias SA, and Esselman PC. Mitochondrial oxidative capacity in vivo declines with age in human muscle. *Faseb J* 14: A49-A49, 2000.

40. Conley KE, Jubrias SA, and Esselman PC. Oxidative capacity and ageing in human muscle. *J Physiol-London* 526: 203-210, 2000.

41. Crow MT, and Kushmerick MJ. Chemical energetics of slow- and fast-twitch muscles of the mouse. *J Gen Physiol* 79: 147-166, 1982.

42. Crowther GJ, Milstein JM, Jubrias SA, Kushmerick MJ, Gronka RK, and Conley KE. Altered energetic properties in skeletal muscle of men with well-controlled insulin-dependent (type 1) diabetes. *Am J Physiol-Endoc M* 284: E655-E662, 2003.

43. Davies KJ, Packer L, and Brooks GA. Biochemical adaptation of mitochondria, muscle, and whole-animal respiration to endurance training. *Arch Biochem Biophys* 209: 539-554, 1981.

44. Davies RE. A Molecular Theory of Muscle Contraction: Calcium-Dependent Contractions with Hydrogen Bond Formation Plus Atp-Dependent Extensions of Part of the Myosin-Actin Cross-Bridges. *Nature* 199: 1068-1074, 1963.

45. Dawson MJ, Gadian DG, and Wilkie DR. Contraction and recovery of living muscles studies by 31P nuclear magnetic resonance. *J Physiol* 267: 703-735, 1977.

46. Dawson MJ, Gadian DG, and Wilkie DR. Muscular fatigue investigated by phosphorus nuclear magnetic resonance. *Nature* 274: 861-866, 1978.

47. De Blasi RA, Almenrader N, Aurisicchio P, and Ferrari M. Comparison of two methods of measuring forearm oxygen consumption (mVO2) by near infrared spectroscopy. *Journal Of Biomedical Optics* 2: 171-175, 1997.

48. De Feyter HM, van den Broek NMA, Praet SFE, Nicolay K, van Loon LJC, and Prompers JJ. Early or advanced stage type 2 diabetes is not accompanied by in vivo skeletal muscle mitochondrial dysfunction. *European Journal Of Endocrinology / European Federation Of Endocrine Societies* 158: 643-653, 2008.

49. Deblasi RA, Ferrari M, Natali A, Conti G, Mega A, and Gasparetto A. Noninvasive Measurement of Forearm Blood-Flow and Oxygen-Consumption by near-Infrared Spectroscopy. *Journal of Applied Physiology* 76: 1388-1393, 1994.

50. Dohm GL, Huston RL, Askew EW, and Fleshood HL. Effects of exercise, training, and diet on muscle citric acid cycle enzyme activity. *Can J Biochem* 51: 849-854, 1973.

51. Dudley GA, Abraham WM, and Terjung RL. Influence of exercise intensity and duration on biochemical adaptations in skeletal muscle. *J Appl Physiol* 53: 844-850, 1982.

52. Dudley GA, Tullson PC, and Terjung RL. Influence of mitochondrial content on the sensitivity of respiratory control. *The Journal of biological chemistry* 262: 9109-9114, 1987.

53. Edwards RHT, Wilkie DR, Dawson MJ, Gordon RE, and Shaw D. Measurement of Muscle Ph and Intermediary Metabolism by P-31 Topical Magnetic-Resonance (Tmr) in Normal Subjects and Patients with Myopathy. *Eur J Clin Invest* 12: 10-10, 1982.

54. Erickson ML, Ryan TE, Young HJ, and McCully KK. Near-infrared assessments of skeletal muscle oxidative capacity in persons with spinal cord injury. *European Journal Of Applied Physiology* [Accepted: April 29, 2013].

55. Evans CL, and Hill AV. The relation of length to tension development and heat production on contraction in muscle. *J Physiol* 49: 10-16, 1914.

56. Fenn WO. A quantitative comparison between the energy liberated and the work performed by the isolated sartorius muscle of the frog. *The Journal of physiology* 58: 175-203, 1923.

57. Fenn WO. The relation between the work performed and the energy liberated in muscular contraction. *The Journal of physiology* 58: 373-395, 1924.

58. Ferrari M, Mathalib M, and Quaresima V. The use of near-infrared spectroscopy in understanding skeletal muscle physiology: recent developments. *Philos Transact A Math Phys Eng Sci* 369: 4577-4590, 2011.

59. Ferreira LF, Townsend DK, Lutjemeier BJ, and Barstow TJ. Muscle capillary blood flow kinetics estimated from pulmonary O2 uptake and near-infrared spectroscopy. *Journal of Applied Physiology* 98: 1820-1828, 2005.

60. Forbes SC, Raymer GH, Kowalchuk JM, Thompson RT, and Marsh GD. Effects of recovery time on phosphocreatine kinetics during repeated bouts of heavy-intensity exercise. *European Journal Of Applied Physiology* 103: 665-675, 2008.

61. Forbes SC, Slade JM, Francis RM, and Meyer RA. Comparison of oxidative capacity among leg muscles in humans using gated 31P 2-D chemical shift imaging. *NMR In Biomedicine* 22: 1063-1071, 2009.

62. Forbes SC, Slade JM, and Meyer RA. Short-term high-intensity interval training improves phosphocreatine recovery kinetics following moderate-intensity exercise in humans. *Applied Physiology, Nutrition, And Metabolism* 33: 1124-1131, 2008.

63. Gnaiger E. Bioenergetics at low oxygen: dependence of respiration and phosphorylation on oxygen and adenosine diphosphate supply. *Resp Physiol* 128: 277-297, 2001.

64. Gnaiger E. Capacity of oxidative phosphorylation in human skeletal muscle: new perspectives of mitochondrial physiology. *Int J Biochem Cell Biol* 41: 1837-1845, 2009.

65. Grassi B, Pogliaghi S, Rampichini S, Quaresima V, Ferrari M, Marconi C, and Cerretelli P. Muscle oxygenation and pulmonary gas exchange kinetics during cycling exercise on-transitions in humans. *Journal of Applied Physiology* 95: 149-158, 2003.

66. Gray MW, Burger G, and Lang BF. Mitochondrial evolution. *Science* 283: 1476-1481, 1999.

67. Haldane J. The Detection and Estimation of Carbonic Oxide in Air. *The Journal of physiology* 20: 521-522, 1896.

68. Haldane J. A Method of Detecting and Estimating Carbonic Oxide in Air. *The Journal of physiology* 18: 463-469, 1895.

69. Haldane J. A new form of Apparatus for measuring the Respiratory Exchange of Animals. *The Journal of physiology* 13: 419-430, 1892.

70. Haldane J. A rapid Method of determining Carbonic Acid in Air. *J Hyg (Lond)* 1: 109-114, 1901.

71. Haldane J. Some Improved Methods of Gas Analysis. *The Journal of physiology* 22: 465-480, 1898.

72. Haldane J. The supposed oxidation of carbonic oxide in the living body. *The Journal of physiology* 25: 225-229, 1900.

73. Haldane JS. A Convenient Form of Gas Analysis Apparatus. *J Hyg (Lond)* 6: 74-76, 1906.

74. Hamaoka T, McCully KK, Quaresima V, Yamamoto K, and Chance B. Near-infrared spectroscopy/imaging for monitoring muscle oxygenation and oxidative metabolism in healthy and diseased humans. *Journal Of Biomedical Optics* 12: 062105-062105, 2007.

75. Harkema SJ, Adams GR, and Meyer RA. Acidosis has no effect on the ATP cost of contraction in cat fast- and slow-twitch skeletal muscles. *American Journal of Physiology - Cell Physiology* 272: C485-C490, 1997.

76. Hartree W, and Hill AV. The recovery heat-production in muscle. *J Physiol* 56: 367-381, 1922.

77. Haseler LJ, Hogan MC, and Richardson RS. Skeletal muscle phosphocreatine recovery in exercise-trained humans is dependent on O-2 availability. *Journal of Applied Physiology* 86: 2013-2018, 1999.

78. Haseler LJ, Lin A, Hoff J, and Richardson RS. Oxygen availability and PCr recovery rate in untrained human calf muscle: evidence of metabolic limitation in normoxia. *American Journal Of Physiology Regulatory, Integrative And Comparative Physiology* 293: R2046-R2051, 2007.

79. He ZH, Bottinelli R, Pellegrino MA, Ferenczi MA, and Reggiani C. ATP consumption and efficiency of human single muscle fibers with different myosin isoform composition. *Biophys J* 79: 945-961, 2000.

80. Hebert SL, Lanza IR, and Nair KS. Mitochondrial DNA alterations and reduced mitochondrial function in aging. *Mech Ageing Dev* 131: 451-462, 2010.

81. Hill AV. The Effect of Load on the Heat of Shortening of Muscle. *Proc R Soc Lond B Biol Sci* 159: 297-318, 1964.

82. Hill AV. The energetics of relaxation in a muscle twitch. *Proc R Soc Lond B Biol Sci* 136: 211-219, 1949.

83. Hill AV. The heat of activation and the heat of shortening in a muscle twitch. *Proc R Soc Lond B Biol Sci* 136: 195-211, 1949.

84. Hill AV. The heat produced by a muscle after the last shock of a tetanus. *J Physiol* 159: 518-545, 1961.

85. Hill AV. The heat-production in prolonged contractions of an isolated frog's muscle. *J Physiol* 47: 305-324, 1913.

86. Hill AV. Length of muscle, and the heat and tension developed in an isometric contraction. *J Physiol* 60: 237-263, 1925.

87. Hill AV. The priority of the heat production in a muscle twitch. *Proc R Soc Lond B Biol Sci* 148: 397-402, 1958.

88. Hill AV. Work and heat in a muscle twitch. *Proc R Soc Lond B Biol Sci* 136: 220-228, 1949.

89. Hill AV, and Hartree W. The four phases of heat-production of muscle. *J Physiol* 54: 84-128, 1920.

90. Holloszy JO. Biochemical adaptations in muscle. Effects of exercise on mitochondrial oxygen uptake and respiratory enzyme activity in skeletal muscle. *The Journal of biological chemistry* 242: 2278-2282, 1967.

91. Iotti S, Lodi R, Frassineti C, Zaniol P, and Barbiroli B. In-Vivo Assessment of Mitochondrial Functionality in Human Gastrocnemius-Muscle by P-31 Mrs - the Role of Ph in the Evaluation of Phosphocreatine and Inorganic-Phosphate Recoveries from Exercise. *NMR In Biomedicine* 6: 248-253, 1993.

92. Isbell DC, Berr SS, Toledano AY, Epstein FH, Meyer CH, Rogers WJ, Harthun NL, Hagspiel KD, Weltman A, and Kramer CM. Delayed calf muscle phosphocreatine recovery after exercise identifies peripheral arterial disease. *Journal Of The American College Of Cardiology* 47: 2289-2295, 2006.

93. Jobsis FF. Noninvasive, infrared monitoring of cerebral and myocardial oxygen sufficiency and circulatory parameters. *Science* 198: 1264-1267, 1977.

94. Joseph A-M, Joanisse DR, Baillot RG, and Hood DA. Mitochondrial dysregulation in the pathogenesis fo diabetes: Potential for mitochondrial biogenesis-mediated interventions. *Experimental Diabetes Research* 2012: 2012.

95. Joseph AM, Joanisse DR, Baillot RG, and Hood DA. Mitochondrial dysregulation in the pathogenesis of diabetes: potential for mitochondrial biogenesis-mediated interventions. *Exp Diabetes Res* 2012: 642038, 2012.

96. KENT-BRAUN JA, MILLER RG, and WEINER MW. Human Skeletal Muscle Metabolism in Health and Disease: Utility of Magnetic Resonance Spectroscopy. *Exercise and Sport Sciences Reviews* 23: 305-348, 1995.

97. Kent-Braun JA, and Ng AV. Skeletal muscle oxidative capacity in young and older women and men. *Journal of Applied Physiology* 89: 1072-1078, 2000.

98. Kent-Braun JA, Sharma KR, Miller RG, and Weiner MW. Postexercise phosphocreatine resynthesis is slowed in multiple sclerosis. *Muscle Nerve* 17: 835-841, 1994.

99. Koenigsberger L. *Hermann von Helmholtz*. Oxford: Clarendon Press, 1906, p. 436.

100. Kowalchuk JM, Rossiter HB, Ward SA, and Whipp BJ. The effect of resistive breathing on leg muscle oxygenation using near-infrared spectroscopy during exercise in men. *Exp Physiol* 87: 601-611, 2002.

101. Krebs HA. Control of metabolism. *Exp Eye Res* 1: 350-353, 1962.

102. Krebs HA. Intermediary metabolism of animal tissue between 1911 and 1969. *Biochem Soc Symp* 30: 123-136, 1970.

103. Krebs HA, and Eggleston LV. Metabolism of acetoacetate in animal tissues. *The Biochemical journal* 42: 294-305, 1948.

104. Krebs HA, and Eggleston LV. Metabolism of acetoacetate in animal tissues. *The Biochemical journal* 39: 408-419, 1945.

105. Krebs HA, and Eggleston LV. Metabolism of acetoacetate in animal tissues. 1. *The Biochemical journal* 39: 408-419, 1945.

106. Krebs HA, and Eggleston LV. Metabolism of acetoacetate in animal tissues. 2. *The Biochemical journal* 42: 294-305, 1948.

107. Lanza IR, and Nair KS. Muscle mitochondrial changes with aging and exercise. *Am J Clin Nutr* 89: 467S-471S, 2009.

108. Larsen FJ, Schiffer TA, Borniquel S, Sahlin K, Ekblom B, Lundberg JO, and Weitzberg E. Dietary inorganic nitrate improves mitochondrial efficiency in humans. *Cell Metab* 13: 149-159, 2011.

109. Larson-Meyer DE, Newcomer BR, Hunter GR, Joanisse DR, Weinsier RL, and Bamman MM. Relation between in vivo and in vitro measurements of skeletal muscle oxidative metabolism. *Muscle Nerve* 24: 1665-1676, 2001.

110. Layec G, Bringard A, Le Fur Y, Vilmen C, Micallef JP, Perrey S, Cozzone PJ, and Bendahan D. Reproducibility Assessment of Metabolic Variables Characterizing Muscle Energetics In Vivo: A P-31-MRS Study. *Magn Reson Med* 62: 840-854, 2009.

111. Levy M, Kushnir T, Mizrahi J, and Itzchak Y. In vivo 31P NMR studies of paraplegics' muscles activated by functional electrical stimulation. *Magnetic resonance in medicine : official journal of the Society of Magnetic Resonance in Medicine / Society of Magnetic Resonance in Medicine* 29: 53-58, 1993.

112. Lodi R, Hart PE, Rajagopalan B, Taylor DJ, Crilley JG, Bradley JL, Blamire AM, Manners D, Styles P, Schapira AH, and Cooper JM. Antioxidant treatment improves in vivo cardiac and skeletal muscle bioenergetics in patients with Friedreich's ataxia. *Ann Neurol* 49: 590-596, 2001.

113. Lodi R, Taylor DJ, and Schapira AH. Mitochondrial dysfunction in friedreich's ataxia. *Biol Signals Recept* 10: 263-270, 2001.

114. Malagoni AM, Felisatti M, Mandini S, Mascoli F, Manfredini R, Basaglia N, Zamboni P, and Manfredini F. Resting muscle oxygen consumption by near-infrared spectroscopy in peripheral arterial disease: A parameter to be considered in a clinical setting? *Angiology* 61: 530-536, 2010.

115. Martin TP, Stein RB, Hoeppner PH, and Reid DC. Influence of Electrical-Stimulation on the Morphological and Metabolic Properties of Paralyzed Muscle. *Journal of Applied Physiology* 72: 1401-1406, 1992.

116. Mccully K, Vandenborne K, Walter G, Posner J, and Leigh J. Comparison of Muscle Metabolism between the Lateral and Medial Gastrocnemius. *Faseb J* 6: A963-A963, 1992.

117. McCully KK, Boden BP, Tuchler M, Fountain MR, and Chance B. Wrist flexor muscles of elite rowers measured with magnetic resonance spectroscopy. *Journal of Applied Physiology* 67: 926-932, 1989.

118. McCully KK, Fielding RA, Evans WJ, Leigh JS, Jr., and Posner JD. Relationships between in vivo and in vitro measurements of metabolism in young and old human calf muscles. *Journal Of Applied Physiology (Bethesda, Md: 1985)* 75: 813-819, 1993.

119. Mccully KK, Forciea MA, Hack LM, Donlon E, Wheatley RW, Oatis CA, Goldberg T, and Chance B. Muscle Metabolism in Older Subjects Using P-31 Magnetic-Resonance Spectroscopy. *Can J Physiol Pharm* 69: 576-580, 1991.

120. McCully KK, and Hamaoka T. Near-infrared spectroscopy: what can it tell us about oxygen saturation in skeletal muscle? *Exercise and Sport Sciences Reviews* 28: 123-127, 2000.

121. Mccully KK, Kakihira H, Vandenborne K, and Kentbraun J. Noninvasive Measurements of Activity-Induced Changes in Muscle Metabolism. *J Biomech* 24: 153-161, 1991.

122. McCully KK, Mulcahy TK, Ryan TE, and Zhao Q. Skeletal muscle metabolism in individuals with spinal cord injury. *Journal of Applied Physiology* 111: 143-148, 2011.

123. Mccully KK, Vandenborne K, Demeirleir K, Posner JD, and Leigh JS. Muscle Metabolism in Track Athletes, Using P-31 Magnetic-Resonance Spectroscopy. *Can J Physiol Pharm* 70: 1353-1359, 1992.

124. Meyer RA. A Linear-Model of Muscle Respiration Explains Monoexponential Phosphocreatine Changes. *Am J Physiol* 254: C548-C553, 1988.

125. Meyer RA, and Foley JM. *Cellular processes intergrating the metabolic response to exercise.* New York: Oxford University, 1996.

126. Meyer RA, Sweeney HL, and Kushmerick MJ. A simple analysis of the "phosphocreatine shuttle". *The American Journal Of Physiology* 246: C365-377, 1984.

127. Meyerhof O. Recent Investigations on the Aerobic and an-Aerobic Metabolism of Carbohydrates. *J Gen Physiol* 8: 531-542, 1927.

128. Mitchell P. Coupling of phosphorylation to electron and hydrogen transfer by a chemi-osmotic type of mechanism. *Nature* 191: 144-148, 1961.

129. Mogensen M, Sahlin K, Fernstrom M, Glintborg D, Vind BF, Beck-Nielsen H, and Hojlund K. Mitochondrial respiration is decreased in skeletal muscle of patients with type 2 diabetes. *Diabetes* 56: 1592-1599, 2007.

130. Motobe M, Murase N, Osada T, Homma T, Ueda C, Nagasawa T, Kitahara A, Ichimura S, Kurosawa Y, Katsumura T, Hoshika A, and Hamaoka T. Noninvasive

monitoring of deterioration in skeletal muscle function with forearm cast immobilization and the prevention of deterioration. *Dyn Med* 3: 2, 2004.

131. Nioka S, Kime R, Sunar U, Im J, Izzetoglu M, Zhang J, Alacam B, and Chance B. A novel method to measure regional muscle blood flow continuously using NIRS kinetics information. *Dynamic Medicine: DM* 5: 5-5, 2006.

132. Paganini AT, Foley JM, and Meyer RA. Linear dependence of muscle phosphocreatine kinetics on oxidative capacity. *Am J Physiol-Cell Ph* 272: C501-C510, 1997.

133. Pilegaard H, Saltin B, and Neufer PD. Exercise induces transient transcriptional activation of the PGC-1alpha gene in human skeletal muscle. *J Physiol* 546: 851-858, 2003.

134. Rall JA. Energetic aspects of skeletal muscle contraction: implications of fiber types. *Exercise and Sport Sciences Reviews* 13: 33-74, 1985.

135. Reichmann H, Hoppeler H, Mathieu-Costello O, von Bergen F, and Pette D. Biochemical and ultrastructural changes of skeletal muscle mitochondria after chronic electrical stimulation in rabbits. *Pflugers Arch* 404: 1-9, 1985.

136. Ryan TE, Erickson ML, Brizendine JT, Young HJ, and McCully KK. Noninvasive evaluation of skeletal muscle mitochondrial capacity with near-infrared spectroscopy: correcting for blood volume changes. *Journal of Applied Physiology* 113: 175-183, 2012.

137. Ryschon TW, Fowler MD, Wysong RE, Anthony A, and Balaban RS. Efficiency of human skeletal muscle in vivo: comparison of isometric, concentric, and eccentric muscle action. *Journal of Applied Physiology* 83: 867-874, 1997.

138. Sako T, Hamaoka T, Higuchi H, Kurosawa Y, and Katsumura T. Validity of NIR spectroscopy for quantitatively measuring muscle oxidative metabolic rate in exercise. *Journal of Applied Physiology* 90: 338-344, 2001.

139. Saltin B, and Gollnick PD. *Skeletal muscle adaptability: significance for metabolism and performance*. Bethesda: American Physiological Society.

140. Scelsi R, Marchetti C, Poggi P, Lotta S, and Lommi G. Muscle fiber type morphology and distribution in paraplegic patients with traumatic cord lesion. Histochemical and ultrastructural aspects of rectus femoris muscle. *Acta Neuropathol* 57: 243-248, 1982.

141. Schrauwen-Hinderling VB, Kooi ME, Hesselink MKC, Jeneson JAL, Backes WH, van Echteld CJA, van Engelshoven JMA, Mensink M, and Schrauwen P. Impaired in vivo mitochondrial function but similar intramyocellular lipid content in patients with type 2 diabetes mellitus and BMI-matched control subjects. *Diabetologia* 50: 113-120, 2007.

142. Van Beekvelt MC, Colier WN, Wevers RA, and Van Engelen BG. Performance of near-infrared spectroscopy in measuring local O(2) consumption and blood flow in skeletal muscle. *Journal of Applied Physiology* 90: 511-519, 2001.

143. Van Beekvelt MCP, Borghuis MS, Engelen BGM, Wevers RA, and Colier WN. Adipose tissue thickness affects in vivo quantitative near-IR spectroscopy in human skeletal muscle. *Clin Sci* 101: 21-28, 2001.

144. Vorgerd M, Schols L, Hardt C, Ristow M, Epplen JT, and Zange J. Mitochondrial impairment of human muscle in Friedreich ataxia in vivo. *Neuromuscul Disord* 10: 430-435, 2000.

145. Walter G, Vandenborne K, McCully KK, and Leigh JS. Noninvasive measurement of phosphocreatine recovery kinetics in single human muscles. *Am J Physiol-Cell Ph* 41: C525-C534, 1997.

146. Warburg O. Iron, the Oxygen-Carrier of Respiration-Ferment. *Science* 61: 575-582, 1925.

147. Warburg O. On respiratory impairment in cancer cells. *Science* 124: 269-270, 1956.

148. Warburg O. On the origin of cancer cells. *Science* 123: 309-314, 1956.

149. Warburg O, Wind F, and Negelein E. The Metabolism of Tumors in the Body. *J Gen Physiol* 8: 519-530, 1927.

150. Wright DC, Han DH, Garcia-Roves PM, Geiger PC, Jones TE, and Holloszy JO. Exercise-induced mitochondrial biogenesis begins before the increase in muscle PGC-1alpha expression. *J Biol Chem* 282: 194-199, 2007.

151. Young JC, Chen M, and Holloszy JO. Maintenance of the adaptation of skeletal muscle mitochondria to exercise in old rats. *Med Sci Sport Exer* 15: 243-246, 1983.

CHAPTER 3

TRAINING- AND DETRAINING-INDUCED CHANGES IN SKELETAL MUSCLE METABOLISM WITH OPTICAL SPECTROSCOPY[1]

[1]Ryan, T.E., Southern, W.M., Brizendine, J.T., McCully,K.K. Accepted in *Medicine and Science in Sports and Exercise.*

Abstract

Purpose: Previous studies have used near-infrared spectroscopy (NIRS) to measure skeletal muscle mitochondrial capacity. This study tested the hypothesis that NIRS measured mitochondrial capacity would improve with endurance exercise training and decline with detraining. **Methods:** Nine, young, participants performed four weeks of progressively increasing endurance exercise training of the wrist flexor muscles followed by approximately five weeks of inactivity. The rate of recovery of muscle oxygen consumption (mVO_2) was measured with NIRS every 3-7 days, indicating mitochondrial oxidative capacity. **Results:** A linear increase in mitochondrial capacity (NIRS rate constant) was found with a group average of 64 ± 37% improvement after four weeks of exercise training ($p < 0.05$). Mitochondrial capacity declined exponentially upon cessation of exercise training, with a mean half-time of ~7.7 days. **Conclusion:** Both the magnitude and time course of mitochondrial adaptations to exercise training and detraining measured with NIRS was consistent with previous studies using both in vitro and in vivo techniques. These findings show that NIRS based measurements can detect meaningful changes in mitochondrial capacity.

Keywords:

NIRS, mitochondrial capacity, oxidative metabolism, endurance training, detraining

Introduction

The effects of exercise training on skeletal muscle mitochondrial oxidative capacity have been well-known for a number of years (21). Skeletal muscle contractile activity initiates several cellular signals that results in increased nuclear and mitochondrial gene transcription, followed by translation into mitochondrial proteins (24). Over time, repeated bouts of exercise results in increased mitochondrial enzyme concentrations and activities (14, 19, 23), which have been termed mitochondrial biogenesis. In contrast, a lack of physical activity, aging, and several pathological conditions are associated with reduced mitochondrial function (28, 29, 31).

Historically, skeletal muscle mitochondrial function has been measured using muscle tissue samples that require surgical removal (21-23). The concentration and activity levels of key mitochondrial enzymes such as citrate synthase or succinate dehydrogenase are commonly used as a measure of mitochondrial function (14, 19, 23). A major limitation of these assays is that mitochondrial function is inferred from a very small amount of tissue and the evaluation of a single mitochondrial enzyme. High-resolution respirometry can provide more information about the specific function of the various complexes in the electron transport chain, but the isolated tissue used is subjected to non-physiological conditions (i.e. higher oxygen concentrations). Non-invasive assessments of mitochondrial function have advantages for testing human subjects. In vivo techniques allow for repeated measurements with little, if any, discomfort while circulatory and other regulatory systems remain intact. Phosphorus magnetic resonance spectroscopy (^{31}P-MRS) is the most commonly used in vivo technique for assessing mitochondrial function (6).

Recent advances in optical spectroscopy have led to improved optical devices and applications for studying muscle physiology (12). Near-infrared spectroscopy (NIRS) has been used to measure various aspects of muscle physiology including: muscle blood flow and perfusion (10), muscle oxygen consumption (9, 10, 33), and muscle oxygenation (1, 15). The recovery of muscle oxygen consumption (mVO_2) after exercise, measured with NIRS, has been used as an index of skeletal muscle oxidative capacity (5, 36). Recently, this method has been improved by correcting for the small changes in observed heme concentrations that often occur during these measurements (38). Recent studies have shown the approach to be reproducible, and that the increase in muscle metabolic rate needed for the study can be produced either voluntary or electrical stimulation (37). Furthermore, a recent study from our lab demonstrated that NIRS measured skeletal muscle mitochondrial capacity of endurance-trained cyclists was higher than sedentary control subjects, and that the relative magnitude of difference in mitochondrial capacity was similar to more established techniques (4).

The purpose of this study was to use NIRS measurements of the recovery rate of mVO_2 after exercise to measure changes in skeletal muscle mitochondrial capacity induced by endurance exercise training and detraining. It was hypothesized that mitochondrial capacity would increase with endurance exercise training, and would return to baseline with detraining.

Materials and Methods

Participants

Nine healthy college-aged men and women volunteered to participate in this study (5M/4F; Age = 23 ± 2.3 yr; Height = 172.4 ± 9.8 cm; Weight = 63.4 ± 12.5 kg). Participants were included if they had not been diagnosed with any chronic disease known to influence muscle metabolism, or were not taking medications that could alter muscle mitochondrial function, or if they were not currently performing forearm exercise training more than one day per week. The study was conducted with the approval of the Institutional Review Board at the University of Georgia (Athens, GA), and was carried out in accordance with the Declaration of Helsinki (2008). All participants gave written, informed consent before testing.

Experimental Design

This was a longitudinal study design where participants performed four weeks of unilateral wrist flexor exercise of the non-dominant arm. The wrist flexor muscles were chosen because they are not involved in locomotion and should be reasonably untrained in comparison to the musculature of the thigh or calf. The dominant arm was not trained and served as the control arm. NIRS measurements of mitochondrial capacity were made every 3-7 days throughout the entire length of the study. Maximal voluntary isometric contractions (MVIC) were performed once per week to determine the appropriate weight for exercise training and testing (~30% MVIC).

Wrist flexion exercise was performed 5 days per week for four weeks (20 total sessions) of the non-dominant arm only. Each session consisted of continuous wrist

flexion exercise for 30 minutes. Participants performed the exercise on a padded, flat surface with the elbow at 90 degrees of flexion. Gloves were provided to prevent any discomfort to the hands or skin. Participants trained with dumbbell weights adjusted to ~30% MVIC. Progressive increases in the contraction frequency occurred as tolerated, with the goal of inducing the largest change in mitochondrial capacity. Participants began training with a contraction frequency of 0.3 – 0.5 Hz (600 - 900 contractions per session) and increases to 1.0 - 1.2 Hz (1800 - 2160 contractions per session). During the final one minute of the each exercise training session, participants performed a high-intensity "sprint", which consisted of performing wrist flexions at a maximal rate. This one-minute period was included in an attempt to maximize the stimulus for mitochondrial biogenesis (11). Following the 20th session of exercise, participants were instructed to not perform any forearm exercise for the remaining duration of the study.

Experimental Procedures

NIRS testing was performed on both the experimental (training) and control arm every 3-7 days throughout both the training and detraining portions of the study. Each participant was placed supine, on a padded table with the tested arm extended (90 degrees from the body). For each testing session, the NIRS protocol was performed on both the control and experimental arm, which last approximately 45 minutes. The NIRS probe was placed over the superficial wrist flexor muscles (flexor carpi radialis, palmaris longus, and flexor carpi ulnaris) approximately 2-3 cm distal to the medial epicondyle of the humerus. A blood pressure cuff (Hokanson SC5, Bellevue, WA) was placed proximally to the elbow joint, and was attached to rapid cuff-inflation system (Hokanson E20 cuff

inflator, Bellevue, WA) powered by a 30-gallon commercial air compressor (Husky VT6315, Kenosha, WI).

NIRS signals were obtained using a continuous wave NIRS device (Oxymon MK III, Artinis Medical Systems, The Netherlands), which consisted of 2 channels (2 equivalent pulsed light sources, 2 avalanche photodiode detectors, shielding from ambient light), uses intensity-modulated light at a frequency of 1 MHz and laser diodes at 3 wavelengths (905, 850, and 770 nm) corresponding to the absorption wavelengths of oxyhemoglobin (O_2Hb) and deoxyhemoglobin (HHb), with an autosensing power supply (approximately 40 W at 110-240 V). The probe was set for one source-detector separation distances after measurement of adipose tissue thickness. The source-detector distance was set to the closest available distance (choices available were 25, 30, 35, 40, 45, and 50 mm) that was at least twice the adipose tissue thickness. Adipose tissue thickness (ATT) was measured at the site of the NIRS probe using B-mode ultrasound (LOGIQe; GE HealthCare, USA). NIRS data was collected at 10 Hz. NIRS signals that represent oxygenated (O_2Hb) and deoxygenated (HHb) hemoglobin/myoglobin were corrected for blood volume changes as previously described (38). Once corrected, the $Hb_{difference}$ signal was calculated from the difference of O_2Hb and HHb, which effectively increases the signal (i.e. change in NIRS signal during arterial occlusion) by a factor of two.

NIRS Measurements

The NIRS protocol used was based on a previous study (4). All NIRS measurements were made using the calculated using the $Hb_{difference}$ signal (difference between O_2Hb and HHB, after correction for blood volume shifts). Resting muscle oxygen consumption (mVO_2) was measured as the decline in muscle oxygenation ($Hb_{difference}$ signal) during inflation of a blood pressure cuff to 250 – 300 mmHg. Two resting measurements were made using 30 seconds of arterial occlusion. Resting mVO_2 was calculated using simple linear regression with the first 20 seconds of each occlusion (200 data points). Following the resting measurements, mitochondrial capacity was measured as the rate of recovery of mVO_2 after voluntary wrist flexion exercise. Short duration (~10 seconds) wrist flexion exercise (30% MVIC) was used to increase mVO_2. A series of short duration arterial occlusions was performed immediately following the exercise. The cuff protocol is as follows: cuffs 1-10 = 3 seconds on, 3 seconds off; cuffs 11-15 = 7 seconds on, 7 seconds off; cuffs 16-20 = 10 seconds on, 10 seconds off; cuffs 21+ = 10 seconds on, 20 seconds off. This cuffing protocol was designed to optimize our ability to characterize the recovery of mVO_2 while minimizing any discomfort to the participants. The exercise/cuff protocol was performed twice and the two tests were averaged. An ischemia/hyperemia calibration was used to normalize NIRS signals as previously described (37) . Briefly, 5-seconds of voluntary wrist flexion exercise was performed, followed by inflation of the blood pressure cuff to 250 – 300 mmHg for 3-6 minutes (until the NIRS signals plateau). Upon release of the cuff, a 1-3 minutes period of hyperemia occurs. This calibration was used to scale the NIRS signals to this 'physiological' range.

Calculation of Muscle Oxygen Consumption

mVO_2 was calculated as the slope of change in $Hb_{difference}$ signal during the arterial occlusion using simple linear regression. The post-exercise repeated measurements of mVO_2 were fit to a mono-exponential curve according to the formula below:

$$y(t) = End - Delta * e^{-k \cdot t} \quad \text{(Equation 3.1)}$$

For this equation, *y* represents relative mVO_2 during the arterial occlusion, *End* is the mVO_2 immediately after the cessation of exercise, *Delta* is the change in mVO_2 from rest to end exercise, *t* is time, and *k* is the fitting rate constant. The recovery rate constant (k) of mVO_2 after exercise is proportional to the maximal oxidative capacity.

Statistical Analysis

Data are presented as means ± SD. Statistical analyses were performed using SPSS 19.0 (IBM®, Armonk, NY). A two-way mixed model ANOVA with a within-subjects factor (time) and between-subjects factor (control arm vs. training arm) was performed on the NIRS rate constants. When a significant interaction effect was found, a post hoc analysis was performed using pairwise comparisons of the main effect (time) with a Bonferroni adjustment. An *A Priori* power calculation was performed using G*Power 3 (Heinrich Heine, Düsseldorf, Germany) and yielded a total sample size of 6 based on the interaction term for repeated ANOVA with a 20% improvement in mitochondrial capacity, $\alpha = 0.05$, and power $(1-\beta) = 0.8$.

Results

All participants completed the testing and exercise training without any adverse events. The physical characteristics of the participants in this study are shown in Table 3.1. All participants increased the number of contractions performed throughout the training portion of the study (Session 1 ~ 800 ± 160 contractions, Session 20 ~ 1800 ± 130 contractions; $p < 0.001$). Weekly training progression for the group is shown in Table 3.2. Resting mVO_2 was not altered by training ($p = 0.790$) and was not different between control and training arms (0.29 ± 0.03 vs. 0.31 ± 0.02 %/s, p = 0.461). MVIC did not change over time in either the control arm ($p = 0.833$) or the training arm ($p = 0.537$).

NIRS Mitochondrial Capacity

Representative NIRS raw data and the recovery kinetics of mVO_2 are shown in Figure 3.1a and 3.1b for descriptive purposes. All participants showed improvements in skeletal muscle oxidative capacity in the endurance trained wrist flexors, as indicated by an increase in the rate constant (k) for the recovery of mVO_2 ($p < 0.001$) (Figure 3.2). There was no change in the rate constant (k) in the control arm ($p = 0.757$) (Figure 3.2). The mean coefficient of variation for the NIRS rate constant in the control arm was 10.4% (range = 6 – 16%). We also found that the initial (baseline) NIRS rate constant was not different between the dominant and non-dominant arms (1.17 ± 0.23 vs. 1.15 ± 0.21, $p = 0.717$). The normalized changes in mitochondrial capacity (percent change from baseline) are shown in Figure 3. We found a wide range of improvement in mitochondrial capacity in this study (31 – 151 %). Because of this wide range in

responses to training protocol, we conducted a regression analysis to determine the relationship between the improvement (percent change) and the initial mitochondrial capacity (rate constant at baseline). This relationship was significant [$F(1,8) = 7.447$, $p = 0.029$, $r = -0.718$]. The initial (end-exercise) mVO_2 also increased with exercise training. The initial mVO_2 from the first testing session was 4.45 ± 1.88 %/s and peaked at 6.67 ± 1.34 %/s in testing session 5 ($p = 0.09$).

We also calculated rates of adaptation and de-adaptation in mitochondrial oxidative capacity using the NIRS data. During the exercise training, the mean change in mitochondrial capacity increase linearly over time reaching a peak improvement of approximately 64 ± 37% measured ~48-72 hours after the last training session. Individual training and detraining responses are shown in Table 3.3. Pooled training and detraining responses were characterized with linear regression and monoexponential decay functions respectively (Figure 3.3). A rapid decline in mitochondrial capacity occurred during the detraining portion of the study, which was well-characterized by a monoexponential decay (Figure 3.3). The calculated half-time for the decay in the NIRS rate constant was 7.7 days. There was no significant difference between the starting mitochondrial capacity and mitochondrial capacity after five weeks of detraining ($p = 1.000$).

Discussion

This study found that mitochondrial capacity measured by NIRS improved with exercise endurance training and returned to baseline values with detraining. We are not aware of previous studies that have used the rate constant (k) for the recovery of mVO_2

measured with NIRS to assess training and detrained in skeletal muscle. The magnitude and rate of adaptation in mitochondrial capacity found in this study are in agreement with previous studies that used in vitro measurements from muscle biopsies (14, 16, 18, 19, 21, 39) and in vivo measurements of phosphocreatine resynthesis (13, 35). Moreover, the time course of de-adaptation is also consistent with previous studies (2, 7, 20, 27, 30, 35). The ability to detect training and detrained induced changes support the validity of NIRS based measurements as a technique for assessing mitochondrial oxidative capacity.

In this study, we report a 64 ± 37% increase in mitochondrial oxidative capacity (indicated by the rate constant for the recovery of mVO_2) in response to four weeks of endurance exercise training of the wrist flexor muscles. It is difficult to compare the relative magnitudes of increase in mitochondrial capacity to previous studies due to methodological differences in both the measurement of mitochondrial function and the exercise training protocols. However, the magnitude of change is within the expected range from previous studies. For example, Gollnick et al. (14) reported a 95% increase in succinate dehydrogenase (SDH) activity after 5 months of cycling exercise training in the vastus lateralis muscle. After 2 months of unilateral cycling exercise training, Henriksson et al. (19) reported a 27% increase in SDH activity in the vastus lateralis muscle. Shorter duration exercise training also causes increased mitochondrial function. Spina et al. (39) found that 7-10 days of endurance cycling exercise (~2 hours per day) increased citrate synthase (CS) concentrations by approximately 30% in the vastus lateralis muscle. A similar study by Green and colleagues (18) was published a few years earlier. The authors of this study reported that 10-12 days of endurance exercise increased SDH and CS activities by 14% and 23% respectively in the vastus lateralis

muscle, although these changes were not considered statistically significant. Exercise training-induced increases in mitochondrial capacity have also been reported using the in vivo ^{31}P-MRS (13, 34, 35).

Participants in the current study performed continuous wrist flexion exercise for 30 minutes per day, five days per week, for four weeks. Progressive increases in the exercise intensity were made as tolerated by the participants (~2 ¼ increase in contraction number per training session by the end of the study). The short duration of training, in combination with the increasing stimulus, resulted in a linear increase in mitochondrial capacity during the training portion. This relationship is not unexpected as Green et al. (17) found a linear increase in SDH activity through six weeks of cycling exercise training. Previous studies have suggested that a fixed and unchanging training stimulus might result in a first-order increase in oxidative capacity with a similar rates of adaptation and de-adaptation, which would level off given the appropriate training duration (2, 11, 40).

The participants in this study had a wide range of responses to the exercise training (31% - 151% improvement). The heterogeneity in responses to exercise training was consistent with previous studies suggesting genetic influences on training responses (3). While our study was not designed to determine the mechanisms behind this wide range, several factors could influence the magnitude of change in mitochondrial capacity. We did find a statistically significant relationship between the baseline mitochondrial capacity (NIRS rate constant) and the percent improvement, which accounted for ~50% of the variance in the percent improvement. This suggests that greater improvements were seen in the participants with the lowest rate constant at baseline. Another potential

factor could be differences in the training intensity between participants (11). There were small differences in the number of contractions performed between participants, but all participants increased the number of contractions performed. We did not find a statistically significant relationship between the magnitude of improvement and either the number of contractions performed or the rate of increase in training intensity (i.e. rate of increase in the number of contractions). It is possible that the difference in training intensity between participants was not large enough to detect an effect on the magnitude of adaptation. In addition, there are numerous wrist flexor muscles capable of contributing to the exercise, thus the motor unit recruit patterns (of the superficial wrist flexor muscles where the NIRS device was placed) during training are unknown. We also found no gender differences in the magnitude of improvement in mitochondrial oxidative capacity, consistent with previous reports (32).

Skeletal muscle mitochondrial capacity declined rapidly after the cessation of exercise training. We characterized this decline by fitting the group data to a monoexponential decay function, and calculated the half-time to be 7.7 days. All participants roughly followed this time course, given the expected variation in NIRS rate constants (~10-15%). Both the exponential pattern, and the rate of decline in mitochondrial capacity are consistent with previous studies using *in vitro* techniques. Booth and Holloszy (2) reported half-times for the turnover of cytochrome c in fast and slow rat muscles were 7 and 8 days respectively. This rapid decline in mitochondrial enzyme concentration/activity in human skeletal muscle has been shown to be somewhere between 2 and 6 weeks (7, 20, 25-27, 30).

In the current study, NIRS was used to measure the rate of recovery of muscle oxygen consumption after exercise. The rate constant for the recovery is proportional to mitochondrial oxidative capacity, such that higher rate constants are related to higher maximal rates of oxygen consumption (i.e. State 3 respiration). The relative contributions of myoglobin and hemoglobin to the NIRS signal remains controversial (8). The quantification of NIRS signals, in combination with the approach used in this study should allow for the calculation of a maximal oxidative capacity (in mM O_2/s), similar to calculations utilized with phosphorus magnetic resonance spectroscopy ($Q_{max} = [PCr]_{rest} * k_{PCr}$; where the maximal rate of ATP production is calculated as the rate constant for phosphocreatine recovery times the resting concentration of phosphocreatine).

In conclusion, this study reports changes in skeletal muscle mitochondrial oxidative capacity in response to endurance exercise training and detraining measured in the wrist flexor muscles with near-infrared spectroscopy (NIRS). Both the magnitude and time course of changes in mitochondrial capacity were consistent with previous studies using both *in vitro* and *in vivo* methods. NIRS based assessments of mitochondrial capacity have previously been shown to be reproducible, independent of the type or magnitude of exercise needed to perform the measurements, and to detect differences in training status in cross-sectional studies. In addition, the NIRS measurements are inexpensive, portable, and easy to perform. Future studies could employ NIRS to examine mitochondrial capacity in both research and clinical settings, especially when repeated-measures on human participants are of interest.

Acknowledgements

The authors would like to thank the participants of this study for their enthusiastic commitment to this study.

The results of the present study do not constitute endorsement by the American College of Sports Medicine.

Funding

This study was funded in part by National Institutes of Health Grant (HD-039676) and the University of Georgia Graduate School intramural grants.

Conflict of interest statement

The authors report no conflicts of interest.

Author Contributions

T.E.R. and K.K.M. conception and design of research; T.E.R., W.M.S., and J.T.B. data collection; T.E.R. and W.M.S. data analysis; T.E.R., J.T.B., W.M.S., and K.K.M. interpreted the results of the experiments; T.E.R. drafted the manuscript; T.E.R., W.M.S., J.T.B., and K.K.M. edited and revised the manuscript; T.E.R., W.M.S., J.T.B., and K.K.M. approved the final version of the manuscript.

References

1. Boone J, Koppo K, Barstow TJ, and Bouckaert J. Pattern of deoxy[Hb+Mb] during ramp cycle exercise: influence of aerobic fitness status. *European Journal Of Applied Physiology* 105: 851-859, 2009.

2. Booth FW, and Holloszy JO. Cytochrome c turnover in rat skeletal muscles. *J Biol Chem* 252: 416-419, 1977.

3. Bouchard C, and Rankinen T. Individual differences in response to regular physical activity. *Med Sci Sports Exerc* 33: S446-451; discussion S452-443, 2001.

4. Brizendine JT, Ryan TE, Larson RD, and McCully KK. Skeletal Muscle Metabolism in Endurance Athletes with Near-Infrared Spectroscopy. *Med Sci Sports Exerc* 2012.

5. Buchheit M, Ufland P, Haydar B, Laursen PB, and Ahmaidi S. Reproducibility and sensitivity of muscle reoxygenation and oxygen uptake recovery kinetics following running exercise in the field. *Clin Physiol Funct Imaging* 31: 337-346, 2011.

6. Chance B, Im J, Nioka S, and Kushmerick M. Skeletal muscle energetics with PNMR: personal views and historic perspectives. *NMR In Biomedicine* 19: 904-926, 2006.

7. Chi MM, Hintz CS, Coyle EF, Martin WH, 3rd, Ivy JL, Nemeth PM, Holloszy JO, and Lowry OH. Effects of detraining on enzymes of energy metabolism in individual human muscle fibers. *Am J Physiol* 244: C276-287, 1983.

8. Davis ML, and Barstow TJ. Estimated contribution of hemoglobin and myoglobin to near infrared spectroscopy. *Respir Physiol Neurobiol* 186: 180-187, 2013.

9. De Blasi RA, Almenrader N, Aurisicchio P, and Ferrari M. Comparison of two methods of measuring forearm oxygen consumption (mVO2) by near infrared spectroscopy. *Journal Of Biomedical Optics* 2: 171-175, 1997.

10. Deblasi RA, Ferrari M, Natali A, Conti G, Mega A, and Gasparetto A. Noninvasive Measurement of Forearm Blood-Flow and Oxygen-Consumption by near-Infrared Spectroscopy. *Journal of Applied Physiology* 76: 1388-1393, 1994.

11. Dudley GA, Abraham WM, and Terjung RL. Influence of exercise intensity and duration on biochemical adaptations in skeletal muscle. *J Appl Physiol* 53: 844-850, 1982.

12. Ferrari M, Mathalib M, and Quaresima V. The use of near-infrared spectroscopy in understanding skeletal muscle physiology: recent developments. *Philos Transact A Math Phys Eng Sci* 369: 4577-4590, 2011.

13. Forbes SC, Slade JM, and Meyer RA. Short-term high-intensity interval training improves phosphocreatine recovery kinetics following moderate-intensity exercise in humans. *Applied Physiology, Nutrition, And Metabolism = Physiologie Appliqu√©e, Nutrition Et M√©tabolisme* 33: 1124-1131, 2008.

14. Gollnick PD, Armstrong RB, Saltin B, Saubert CWt, Sembrowich WL, and Shepherd RE. Effect of training on enzyme activity and fiber composition of human skeletal muscle. *J Appl Physiol* 34: 107-111, 1973.

15. Grassi B, Pogliaghi S, Rampichini S, Quaresima V, Ferrari M, Marconi C, and Cerretelli P. Muscle oxygenation and pulmonary gas exchange kinetics during cycling exercise on-transitions in humans. *Journal of Applied Physiology* 95: 149-158, 2003.

16. Green HJ, Helyar R, Ball-Burnett M, Kowalchuk N, Symon S, and Farrance B. Metabolic adaptations to training precede changes in muscle mitochondrial capacity. *J Appl Physiol* 72: 484-491, 1992.

17. Green HJ, Jones S, Ball-Burnett M, Farrance B, and Ranney D. Adaptations in muscle metabolism to prolonged voluntary exercise and training. *J Appl Physiol* 78: 138-145, 1995.

18. Green HJ, Jones S, Ball-Burnett ME, Smith D, Livesey J, and Farrance BW. Early muscular and metabolic adaptations to prolonged exercise training in humans. *J Appl Physiol* 70: 2032-2038, 1991.

19. Henriksson J. Training induced adaptation of skeletal muscle and metabolism during submaximal exercise. *J Physiol* 270: 661-675, 1977.

20. Henriksson J, and Reitman JS. Time course of changes in human skeletal muscle succinate dehydrogenase and cytochrome oxidase activities and maximal oxygen uptake with physical activity and inactivity. *Acta Physiol Scand* 99: 91-97, 1977.

21. Holloszy JO. Biochemical adaptations in muscle. Effects of exercise on mitochondrial oxygen uptake and respiratory enzyme activity in skeletal muscle. *J Biol Chem* 242: 2278-2282, 1967.

22. Holloszy JO, and Booth FW. Biochemical adaptations to endurance exercise in muscle. *Annu Rev Physiol* 38: 273-291, 1976.

23. Holloszy JO, Oscai LB, Don IJ, and Mole PA. Mitochondrial citric acid cycle and related enzymes: adaptive response to exercise. *Biochem Biophys Res Commun* 40: 1368-1373, 1970.

24. Hood DA. Mechanisms of exercise-induced mitochondrial biogenesis in skeletal muscle. *Appl Physiol Nutr Metab* 34: 465-472, 2009.

25. Houmard JA, Hortobagyi T, Johns RA, Bruno NJ, Nute CC, Shinebarger MH, and Welborn JW. Effect of short-term training cessation on performance measures in distance runners. *Int J Sports Med* 13: 572-576, 1992.

26. Houmard JA, Hortobagyi T, Neufer PD, Johns RA, Fraser DD, Israel RG, and Dohm GL. Training cessation does not alter GLUT-4 protein levels in human skeletal muscle. *J Appl Physiol* 74: 776-781, 1993.

27. Houston ME, Bentzen H, and Larsen H. Interrelationships between skeletal muscle adaptations and performance as studied by detraining and retraining. *Acta Physiol Scand* 105: 163-170, 1979.

28. Joseph AM, Joanisse DR, Baillot RG, and Hood DA. Mitochondrial dysregulation in the pathogenesis of diabetes: potential for mitochondrial biogenesis-mediated interventions. *Exp Diabetes Res* 2012: 642038, 2012.

29. KENT-BRAUN JA, MILLER RG, and WEINER MW. Human Skeletal Muscle Metabolism in Health and Disease: Utility of Magnetic Resonance Spectroscopy. *Exercise and Sport Sciences Reviews* 23: 305-348, 1995.

30. Klausen K, Andersen LB, and Pelle I. Adaptive changes in work capacity, skeletal muscle capillarization and enzyme levels during training and detraining. *Acta Physiol Scand* 113: 9-16, 1981.

31. Lanza IR, and Nair KS. Muscle mitochondrial changes with aging and exercise. *Am J Clin Nutr* 89: 467S-471S, 2009.

32. Lewis DA, Kamon E, and Hodgson JL. Physiological differences between genders. Implications for sports conditioning. *Sports Med* 3: 357-369, 1986.

33. Malagoni AM, Felisatti M, Mandini S, Mascoli F, Manfredini R, Basaglia N, Zamboni P, and Manfredini F. Resting muscle oxygen consumption by near-infrared spectroscopy in peripheral arterial disease: A parameter to be considered in a clinical setting? *Angiology* 61: 530-536, 2010.

34. McCully K, and Posner J. Measuring exercise-induced adaptations and injury with magnetic resonance spectroscopy. *International Journal of Sports Medicine* 13 Suppl 1: S147-S149, 1992.

35. Mccully KK, Kakihira H, Vandenborne K, and Kentbraun J. Noninvasive Measurements of Activity-Induced Changes in Muscle Metabolism. *J Biomech* 24: 153-161, 1991.

36. Motobe M, Murase N, Osada T, Homma T, Ueda C, Nagasawa T, Kitahara A, Ichimura S, Kurosawa Y, Katsumura T, Hoshika A, and Hamaoka T. Noninvasive monitoring of deterioration in skeletal muscle function with forearm cast immobilization and the prevention of deterioration. *Dyn Med* 3: 2, 2004.

37. Ryan TE, Brizendine JT, and McCully KK. A comparison of exercise type and intensity on the noninvasive assessment of skeletal muscle mitochondrial function using near-infrared spectroscopy. *J Appl Physiol* 114: 230-237, 2013.

38. Ryan TE, Erickson ML, Brizendine JT, Young HJ, and McCully KK. Noninvasive evaluation of skeletal muscle mitochondrial capacity with near-infrared spectroscopy: correcting for blood volume changes. *Journal of Applied Physiology* 113: 175-183, 2012.

39. Spina RJ, Chi MM, Hopkins MG, Nemeth PM, Lowry OH, and Holloszy JO. Mitochondrial enzymes increase in muscle in response to 7-10 days of cycle exercise. *J Appl Physiol* 80: 2250-2254, 1996.

40. Terjung RL. The turnover of cytochrome c in different skeletal-muscle fibre types of the rat. *Biochem J* 178: 569-574, 1979.

Table 3.1. Physical characteristics of the participants.

	Height *(cm)*	**Weight** *(kg)*	**Age** *(yr)*	**ATT (mm)** *Control Arm*	*Training Arm*
Males (*n* = 5)	178.8 ± 7.3	72.3 ± 5.3	24.0 ± 2.1	3.4 ± 0.4	3.4 ± 0.5
Females (*n* = 4)	164.5 ± 5.6	52.3 ± 9.2	21.8 ± 2.2	5.2 ± 3.1	5.1 ± 3.2
Total (*n* = 9)	172.4 ± 9.8	63.4 ± 12.5	23.0 ± 2.3	4.2 ± 2.1	4.2 ± 2.2

Note: Data presented as means ± SD. Statistical comparisons between genders were not performed.

Table 3.2: Weekly progression in training intensity.

	Week 1	Week 2	Week 3	Week4
Number of Contractions (*n* = 9)	4200 ± 350	5300 ± 450	6500 ± 300	8400 ± 600

Note: Data are presented as means ± SD. The number of contractions performed per week (5 sessions of exercise; each session 30 minutes) was increased throughout the training by increasing the contraction frequency as tolerated.

Table 3.3: Individual responses to exercise training and detraining

Participant Number	Training Response (% Change) *(linear regression)*				Detraining Response (% Change) *(exponential decay)*		
	Slope (m)	Intercept (b)	Magnitude (%)	R^2	k_{decay}	Half-time (days)	R^2
1	8.8	-18.0	151	0.90	0.06	14.4	0.97
2	3.0	-1.1	100	0.86	0.21	6.2	0.99
3	1.8	6.7	53	0.80	0.09	9.9	0.86
4	2.5	-0.6	52	0.99	0.17	6.9	0.99
5	2.1	-3.8	57	0.98	0.11	9.2	0.98
6	2.8	7.3	63	0.82	0.16	7.2	0.77
7	1.6	-3.4	31	0.94	0.16	7.2	0.80
8	2.1	-2.9	48	0.86	0.17	6.9	0.92
9	2.1	-1.5	40	0.97	0.19	6.5	0.85
MEAN	2.9	-1.9	66	0.90	0.15	8.3	0.90
SD	2.2	7.3	37	0.07	0.05	2.6	0.09

Values presented are for each individual participant. Training responses (% change in NIRS rate constant) were fit using simple linear regression. Detraining responses (% change in NIRS rate constant) were fit using a mono-exponential decay. Half-times were calculated from the decay rate constant (k_{decay}) and the time delay between the first detraining measurement and the last exercise session (~2-3 days).

A

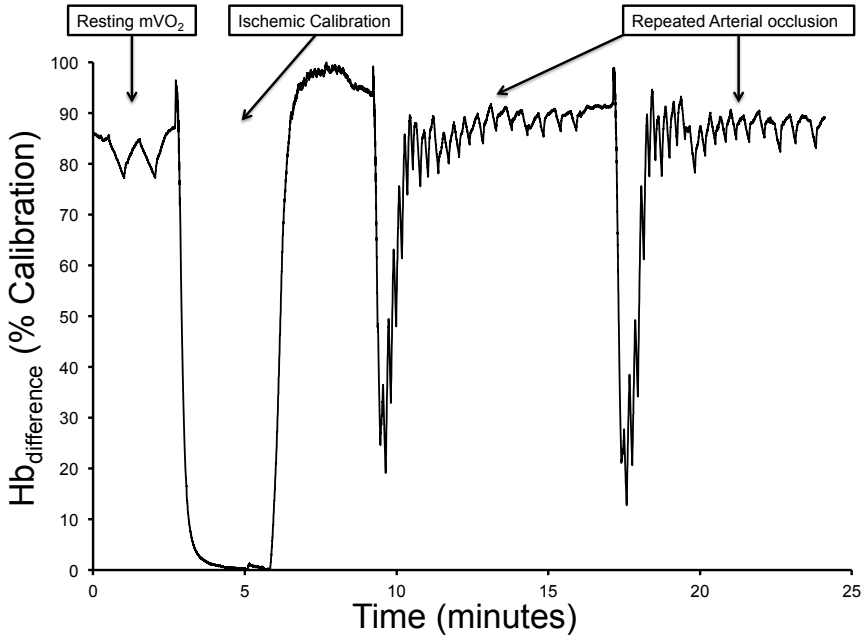

B

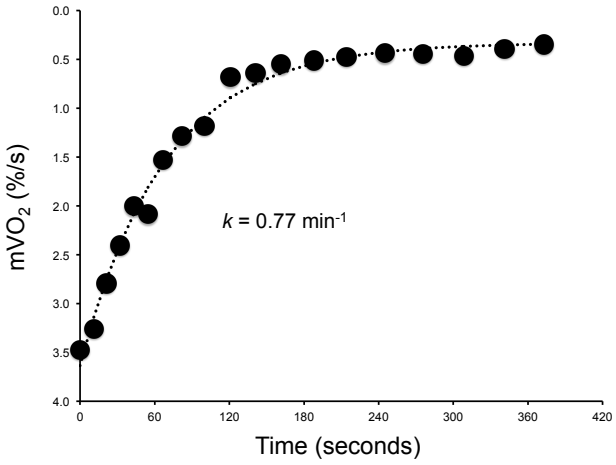

Figure 3.1. A representative testing protocol showing the NIRS $Hb_{difference}$ signal showing resting measurements of mVO_2, an ischemic calibration, and two exercise/recovery trials for the measurement of post-exercise kinetics for mVO_2 is shown in panel A. Each arterial occlusion is fit to a mono-exponential function and the rate constant (proportional to mitochondrial oxidative capacity) is calculated (Panel B)

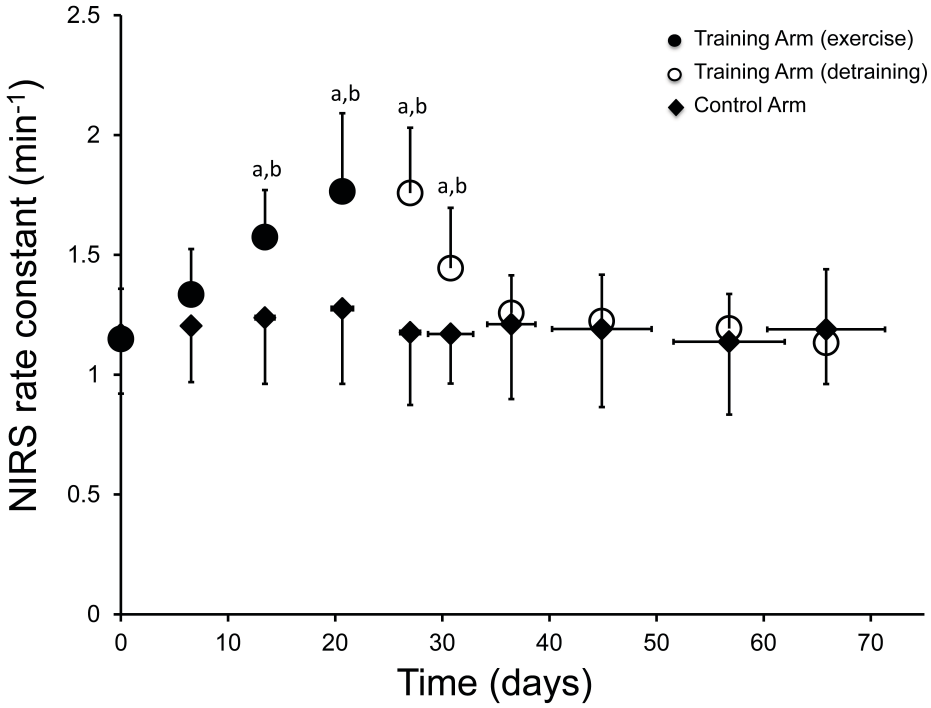

Figure 3.2. NIRS rate constants (k) for the recovery of mVO_2 during exercise training (closed circles) and detraining (open circles). The control arm (closed triangles) did not perform exercise training. [a]Rate constants were statistically different between the training and control arms (all points $p < 0.05$). [b]Rate constants from the training arm were significantly different from the baseline (time = 0 days) at testing sessions 3-6 (all points $p < 0.05$).

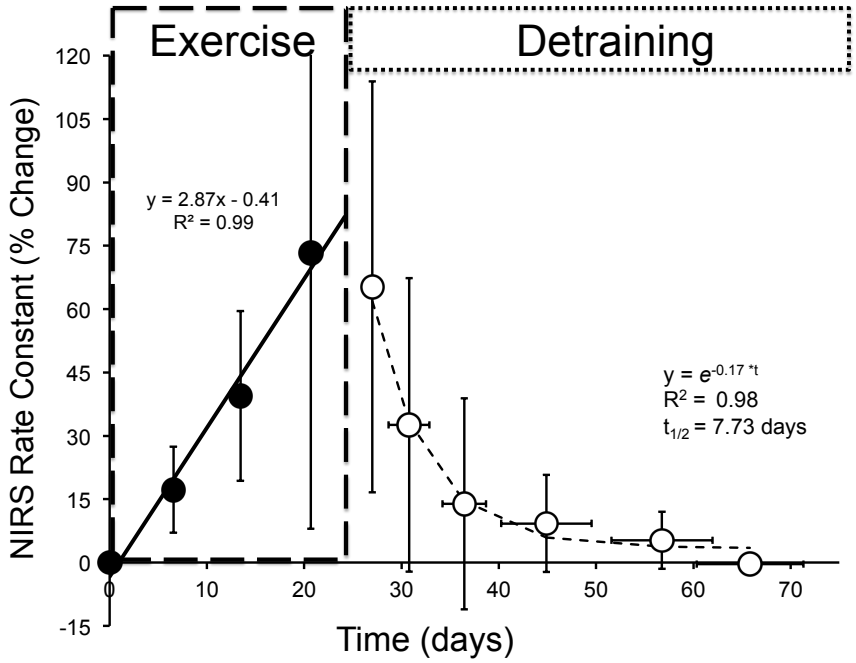

Figure 3.3. Percentage change in NIRS rate constant (proportional to mitochondrial capacity) from baseline (time = 0 days) of the training arm. Data from all participants were averaged prior to the calculation of fitting parameters. Data from the training portion were characterized using simple linear regression. Detraining data were fit to a monoexponential decay function and half-times were calculated ($t_{1/2}$). Data are presented as the mean ± SD (error bars).

CHAPTER 4

VALIDATION OF NEAR INFRARED SPECTROSCOPY MEASUREMENTS OF SKELETAL MUSCLE OXIDATIVE CAPACITY WITH PHOSPHORUS MAGNETIC RESONANCE SPECTROSCOPY[2]

[2]Ryan, T.E., Southern, W.M., Reynolds, M.A., McCully, K.K. To be submitted to the *American Journal of Physiology – Regulatory, Intergrative, and Comparative Physiology.*

Abstract

Purpose: The purpose of this study was to validate measurements of skeletal muscle oxidative capacity made with near infrared spectroscopy (NIRS) measurements to those made with phosphorus magnetic resonance spectroscopy (^{31}P-MRS). **Methods:** Sixteen young (age = 22.5 ± 3.0 years) healthy individuals were testing with both ^{31}P-MRS and NIRS during a single testing visit. The recovery rate of phosphocreatine was measured inside the bore of a 3 tesla MRI scanner, after short duration (10 seconds) plantarflexion execise as an index of skeletal muscle oxidative capacity. Using NIRS, the recovery rate of muscle oxygen consumption (mVO_2) was also measured outside the MRI scanner, after short duration (10 seconds) plantarflexion execise as an index of skeletal muscle oxidative capacity. **Results:** The average recovery time constant was 31.5 ± 8.5 s for PCr and 31.5 ± 8.9 s for mVO_2 ($p = 0.709$). ^{31}P-MRS correlated well with NIRS for both Channel 1 (Pearson's $r = 0.88$, $p < 0.0001$) and Channel 2 (Pearson's $r = 0.95$, $p < 0.0001$). Both ^{31}P-MRS and NIRS exhibit good repeatability between trials (CV = 8.1%, 6.9%, and 7.9% for NIRS Channel 1, NIRS Channel 2, and ^{31}P-MRS respectively). **Conclusion:** The good agreement between NIRS and ^{31}P-MRS indices of skeletal muscle oxidative capacity suggest that NIRS is a valid method for assessing mitochondrial function, and that direct comparisons between NIRS and ^{31}P-MRS measurements may be possible.

Keywords:

NIRS, mitochondrial capacity, MRS, oxidative metabolism, mitochondrial function

Introduction

The mitochondrion is a dual-membrane organelle that is vital for maintaining proper cell function. Mitochondria have several roles including cellular growth and differentiation, apoptosis, and cellular signaling, but are most known for their metabolic capability to generate chemical energy in the form of adenosine triphosphate (25). In skeletal muscle, mitochondria generate most of the fuel required for contractile activity and physical functioning, under normal conditions. Both the number of mitochondria and the function of mitochondria are related to exercise performance (12-14). Reduced mitochondrial function and/or density are also associated with several pathological conditions including diabetes (16, 29), age-associated diseases (6, 22), neuromuscular diseases (17, 20, 23, 38). Because of the importance of mitochondrial function for both health and physical performance, the development of novel, cost-effective methodologies to study mitochondrial health is critical.

Traditionally, mitochondrial function has been studied using methods that can be classified into two categories: invasive (or *in vitro*) or non-invasive (or *in vivo*) approaches. In vitro approaches involve a small biopsy of muscle tissue to measure enzyme concentrations or activity levels (12, 13), or isolated mitochondrial preparations (5), or permeabilized muscle fiber preparations (11). Until recently, *in vivo* approaches to studying mitochondrial function have been limited to the use of magnetic resonance spectroscopy (MRS) to study changes in phosphorus (^{31}P) metabolites during exercise and the recovery post-exercise (4). The most widely used ^{31}P-MRS assessment for mitochondrial function is the recovery rate of phosphocreatine (PCr) following exercise. Using the assumption of equilibrium for the creatine kinase reaction, the recovery rate of

PCr after exercise is a function of mitochondrial ATP production, which has been validated against *in vitro* measurements of enzyme activity (19, 21) and high resolution respirometry (18).

Our lab has recently utilized a novel, *in vivo* approach to measuring skeletal muscle mitochondrial function using near infrared spectroscopy (NIRS) (33). The approach uses NIRS in combination with a rapid cuff inflation system (used to block oxygen delivery and venous return) to measure kinetic changes in skeletal muscle oxygen consumption (mVO_2) after submaximal exercise. Similar to PCr recovery, we believe the recovery of mVO_2 after exercise is a function of mitochondrial ATP production, and therefore can be used as a measure of skeletal muscle oxidative capacity (26). This NIRS approach has been shown to be reproducible (33) and independent of exercise intensity (32), detects the expected differences between untrained and trained individuals (2), as well as paralyzed and non-paralyzed individuals (9), and to track changes in mitochondrial function with exercise training and detraining (34). In the present study, we validated NIRS measurements of skeletal muscle oxidative capacity with ^{31}P-MRS measurements of skeletal muscle oxidative capacity in a sample of young healthy adults. We also assessed the repeatability of both NIRS and ^{31}P-MRS measurements.

Materials and Methods

Participants

Sixteen healthy participants (10 male, 6 female), ages 19 – 30 years, were tested in this study. The study was conducted with the approval of the Institutional Review Board at the University of Georgia (Athens, GA), and all subjects gave written, informed

consent before testing.

Study Design

This study aimed to compare NIRS measurements of skeletal muscle oxidative capacity with ^{31}P-MRS measurements of skeletal muscle oxidative capacity. NIRS and ^{31}P-MRS testing was performed on all participants (in random order) in a single visit to the University of Georgia BioImaging Research Center (Athens, GA). The NIRS and ^{31}P-MRS testing protocols took approximately 30 minutes each. Randomization of NIRS and ^{31}P-MRS was done by coin flip. Seven participants performed ^{31}P-MRS testing first, while the other nine participants performed NIRS testing first.

NIRS Experimental protocol

NIRS testing performed in this study is similar to that describe in previous studies (32, 33). Each subject was placed on a padded table with both legs extended (0° of knee flexion). The participant's dominant foot was placed into a custom-built non-magnetic pneumatic exercise device. The foot was strapped firmly to the exercise device using non-elastic Velcro straps proximal to the base of the fifth digit, and the knee supported. The NIRS optode was placed at the level of the largest circumference of the triceps surae, specifically over the medial head of gastrocnemius muscle, and secured with Velcro straps and biadhesive tape. A blood pressure cuff (Hokanson SC12D; Bellevue, WA) was placed proximal to the NIRS optode above the knee joint. The blood pressure cuff was connected to a rapid-inflation system (Hokanson E20, Bellevue, WA). Adipose tissue thickness (ATT) was measured at the site of the NIRS optode using B-mode ultrasound (LOGIQ e; GE HealthCare, USA). Participants were asked not to consume caffeine or tobacco on the day of the test or to use alcohol or perform moderate or heavy

physical activity for at least 24 hours before the test.

The test protocol consisted two measurements of resting muscle oxygen consumption by way of inflation of a blood pressure cuff (250 - 300 mmHg) for 30 seconds. For the recovery measurements, 10 seconds of plantarflexion exercise was performed at a given resistance (pneumatic resistance in the form of pounds per square inch [PSI]) to increase mVO_2. The resistance was set during a familiarization session prior to testing to a level that would produce the optimal balance between force and speed of contractions. For example, the participants were expected to perform plantarflexions at the highest PSI (air resistance) that would allow for a minimum of 2 contractions per second. Previous studies have shown short duration exercise produces similar initial rates of phosphocreatine resynthesis (39). Following the plantarflexion exercise, a series of 10 - 18 brief (5 - 10 seconds) arterial occlusions were applied to measure the rate of recovery of mVO_2 back to resting levels. There was a small time delay between the end-exercise and initial arterial occlusion (~2 seconds) due to movement of the exercise ergometer as the pressure dissipated from the air cylinder. To maximize our ability to measure the recovery of mVO_2 while minimizing the discomfort to participants, the following cuff protocol was used: 5 seconds on / 5 seconds off for cuffs 1-6, 7 seconds on / 7 seconds off for cuffs 7-10, 10 seconds on / 10 seconds off for cuffs 11-14, and 10 seconds on / 20 seconds off for cuffs 15-18). The exercise and repeated cuffing procedure was repeated a second time, with approximately 5-7 minutes in between the first and second exercise/recovery bouts.

An ischemic calibration procedure was performed prior to the recovery measurements as previously described (32) and used to scale the NIRS O_2Hb, HHb, and $Hb_{difference}$ signals to the maximal physiological range.

NIRS device

NIRS signals were obtained using a continuous wave NIRS device (Oxymon MKIII, Artinis Medical Systems, The Netherlands), which uses intensity-modulated light at a frequency of 1 MHz and laser diodes at 3 wavelengths (905, 850, and 770 nm) corresponding to the absorption wavelengths of oxyhemoglobin (O_2Hb) and deoxyhemoglobin (HHb). The probe was set to have two source-detector separation distances (between 30 – 45 mm), with the smallest source-detector distance set to approximately twice the adipose tissue thickness. The second source-detector distance was always 1 cm greater than the first, thus allowing sampling of slightly deeper portion of muscle. NIRS data were collected at 10 Hz.

Calculation of muscle oxygen consumption

mVO_2 was calculated as the slope of change in the $Hb_{difference}$ signal ($Hb_{difference}$ = O_2Hb – HHb) during the arterial occlusion using simple linear regression. mVO_2 was expressed as a percentage of the ischemic calibration per unit time. This measurement was made at rest and repeated a number of times after exercise. The post-exercise repeated measurements of mVO_2 were fit to a mono-exponential curve according to the formula below:

$$y = End - Delta \times e^{-1/Tc} \qquad \text{(Equation 4.1)}$$

For this equation, *y* represents relative mVO_2 during the arterial occlusion, *End* is the mVO_2 immediately after the cessation of exercise, *Delta* is the change in mVO_2 from rest to end exercise, and *Tc* is the fitting time constant.

Correction for blood volume

NIRS data were analyzed using custom-written routines for Matlab v. 7.13.0.564 (The Mathworks, Natick, MA). NIRS signals were corrected for changes in blood volume using the following method as previously described (33).

Calculation of signal to noise ratio

The quality of NIRS data was determined by calculating a signal-to-noise ratio (SNR). The SNR was calculated for each arterial occlusion on all data. The signal was calculated as the change in the NIRS signal during the chosen measurement period of an arterial occlusion, and is therefore a function of the duration of the occlusion and the rate of oxygen consumption. The noise was calculated as the standard deviation of 600 data points (60 seconds) taken prior to the first resting arterial occlusion.

^{31}P-MRS Experimental Protocol

Subjects were tested in a 3 Tesla whole body magnet (GE Healthcare, Waukesha, WI). A ^{1}H and ^{31}P dual tuned radio-frequency (RF) surface coil (Clinical MR Solutions, Brookfield, WI.) was placed over the triceps surae muscle of the subject's dominant leg. The size of the ^{31}P coil was 13cm x 13cm, placed orthogonal to the ^{1}H coil (two loops, side by side, 20 cm x 20 cm in size). Manual shimming on ^{1}H was applied to get a better signal-to-noise ratio (SNR) and less spectrum distortion, after an auto-

shimming by a pre-scan sequence (all subjects ^{1}H FWHM mean ± SD; 0.60 ± 0.14 ppm). A free induction decay (FID) chemical shift imaging (CSI) pulse sequence was applied to acquire the ^{31}P spectrum with the following scan parameters: repetition time (TR) = 3 seconds, FOV = 8 cm, slice thickness = 8 cm, number of excitation (NEX) = 1, rfpulse = hard. A resting phosphorus scan was performed after shimming, which consisted to 50 FIDs.

Exercise Protocol

Plantarflexion exercise in a custom-built non-magnetic pneumatic ergometer was performed inside the bore of the MRI. Identical resistances (PSI) were used for ^{31}P-MRS and NIRS testing. The exercise protocol consisted of ~45 seconds of rest, followed by 10 seconds of rapid plantarflexion, and ~4 minutes for the measurement of the resynthesis of phosphocreatine. ^{31}P spectra were obtained using the same pulse sequence characteristics described above.

Metabolic calculations

Resting spectra were acquired every 3 seconds until 50 scans are taken. The resulting spectra were phased and summed in a custom analysis program (Winspa, Ronald Meyer, Michigan State University). The summed spectra was apodized using 5 Hz exponential line broadening. The area under the curve for each peak (Pi, PDE, PCr, α ATP, β ATP, and γ ATP) was determined using integration. Absolute concentrations were calculated using the assumed value of 8.2 mM for the gamma ATP peak. Saturation effects were corrected for using fully relaxed spectra collected from four individuals using the same pulse sequence above, except the repetition time was changed to 15 seconds. Muscle pH was calculated using the following equation:

$$pH = 6.77 + \log\left(\left(Pi_{shift} - 3.27\right)/\left(5.68 - Pi_{shift}\right)\right) \quad \text{(Equation 4.2)}$$

where Pi_{shift} is the chemical shift of Pi relative to PCr in parts per million (ppm).

Phosphocreatine Recovery

Phosphocreatine concentrations were determined from the peak heights from individual spectra (temporal resolution of 3 seconds) using custom written routines in Matlab v. 7.13.0.564 (The Mathworks, Natick, MA). Individual spectra were apodized using 2 Hz exponential line broadening, followed by zero filling to 8192 points. Peak heights were determined using the magnitude of each spectra. FWHM of each PCr peak was calculated to ensure no changes in magnetic field homogeneity occurred during the recovery period. PCr peak heights during recovery after exercise were fit to an exponential curve.

$$PCr = \mathrm{PCr_{end}} - \Delta PCr \times e^{-t/Tc} \quad \text{(Equation 4.3)}$$

Where PCr_{end} is the percent PCr immediately after cessation of exercise, ΔPCr is the change in PCr from rest to end exercise, and Tc is the fitting time constant. Vmax was calculated from the rate constant of the PCr recovery curve times the resting PCr concentration.

Calculation of signal to noise ratio

The quality of phosphorus data collected was determined by calculating a signal-to-noise ratio for each individual spectra. The signal was calculated as the peak height of phosphocreatine for each spectra (TR = 3s). After apodization (5Hz exponential filtering), the resulting spectra were zero-filled (from 2048 to 8192 points) and Fourier transformed. The noise was calculated as the standard deviation of the first 3000 data points of the spectra.

Statistical analysis

Data are presented as means ± SD. Test-retest reliability was analyzed using coefficient of variation (CV) and intraclass correlation coefficients (ICC). Relative reliability is related to an individual maintaining his/her position within a sample for repeated measurements. We assessed this type of reliability with the ICC(1,1), which indicates error in measurements as a proportion of the total variance in scores. ICC(1,1) analysis was performed on raw scores using a downloadable spreadsheet (15). The absolute reliability can be described as the degree to which repeated measurements vary for individuals. This was performed by calculating the CV for each subject, which is the SD of measurements recorded during both tests divided by the mean of the two tests. CV was expressed as a percentage. PCr time constants were compared to NIRS time constants using a two-tailed Student's *t*-test for paired samples. Statistical analyses were performed using SPSS 19.0 (IBM®, Armonk, NY). Significance was accepted when $p < 0.05$.

Results

All participants completed testing without any adverse events. The physical characteristics of the participants are shown in Table 1. We found no order effects for either ^{31}P-MRS or NIRS in all subsequent statistical analyses (all $p > 0.30$).

NIRS

The resting value for mVO_2 was 0.26 ± 0.10 %/s for all participants. The average time constant for the recovery of mVO_2 after exercise was 31.5 ± 8.9 seconds. The group average recovery of mVO_2 is shown in Figure 1, overlapped with the recovery of PCr. The time constant was reproducible between trials for both channels of NIRS device (CV

= 8.1% and 6.1%, ICC = 0.93 and 0.95; for Channel 1 and Channel 2 respectively). The trials were also well correlated with each other for Channel 1(Pearson's $r = 0.93$, $p < 0.0001$) and Channel 2 (Pearson's $r = 0.94$, $p < 0.0001$) (Figure 2c and 2e). Corresponding Bland-Altman plots for the trials of NIRS Channel 1 and Channel 2 are shown in Figure 2d and 2e respectively. There was no evidence of changes in variance across the range of data ($R^2 < 0.05$, $p > 0.364$) for both NIRS Ch1 and Ch2 using the Bland Altman plot). We also found no gender effects between trials ($p = 0.404$ an $p = 0.728$ for Ch1 and Ch2 respectively). Statistical values regarding the repeatability of NIRS measurements are shown in Table 3. The SNR for NIRS measurements of mVO_2 decreased as mVO_2 returned to resting levels (Figure 4). The average SNR for resting mVO_2 was 7.38 ± 7.06 for Channel 1 and 6.34 ± 5.94 for Channel 2. We did not find a significant relationship between the SNR and adipose tissue thickness ($R^2 = 0.13$, $p = 0.177$).

^{31}P-MRS

The resting and end-exercise values for [PCr] and pH are shown in Table 2. For recovery measurements, we chose to analyze changes in [PCr] as a change in the peak height, rather than using peak fitting algorithms to determine the area under the peak. The assumption that changes in peak height represent changes in concentration is only valid when there is no change in the peak widths (full width half maximum, FWHM). FWHM of PCr was calculated for each spectra, on all tests, and did not change throughout the recovery from exercise (data not shown). The reproducibility of peak heights analysis was determined from the resting scan (50 spectra per participant). The mean CV of PCr peak heights was 1.3 ± 0.7% (range = 0.6 – 2.9%). The average SNR of

resting phosphorus spectra was 154 ± 47. During the recovery of PCr, the SNR increased as PCr is resynthesized (Figure 5).

The average recovery time constant for PCr was 31.5 ± 8.5 s for all participants. The recovery rate was reproducible between trials (CV = 7.6%, ICC = 0.90). Comparisons between trials for the PCr recovery time constant are shown in Figure 2a. The corresponding Bland-Atlman plot is shown in Figure 2b. There was no evidence of changes in variance across the range of data ($R^2 = 0.08$, $p = 0.261$ for Bland Altman plot). We also found no gender effects between trials ($p = 0.629$). During the 10 seconds of rapid plantarflexion exercise [PCr] decreased by ~24%. This short duration exercise bout was designed to deplete PCr without cause significant acidosis. The end-exercise pH was 7.01 ± 0.07. The calculated oxidative capacity ($[PCr]_{resting} * k_{PCr}$; where $PCr_{resting}$ is the resting concentration of PCr and k_{PCr} is the rate constant for the recovery of PCr after exercise) was 1.04 ± 0.28 mM ATP/s.

Relationship between NIRS and ^{31}P-MRS

The rate of recovery of mVO_2 measured by NIRS correlated well with the rate of recovery of PCr measured by ^{31}P-MRS. Using the average time constant for both trials, ^{31}P-MRS correlated well with NIRS for both Channel 1 (Pearson's $r = 0.88$, $p < 0.0001$) and Channel 2 (Pearson's $r = 0.95$, $p < 0.0001$) (Figures 3a and 3b). Bland-Altman plots (Figure 3b and 3c) of the time constants show that the errors (differences between NIRS and ^{31}P-MRS time constants) were approximately symmetrically distributed around zero, with no indication of a systematic bias between measurement techniques. There was no evidence that the level agreement changed over the range of the current data set ($R^2 < 0.04$, $p = 0.438$ for NIRS Ch1 and $R^2 < 0.02$, $p = 0.592$ for NIRS Ch2). We also found no

gender effects for the relationship between ^{31}P-MRS and NIRS Channel 1 ($p = 0.327$) or NIRS Channel 2 ($p = 0.967$).

Discussion

This study found that NIRS-measured recovery rates of muscle oxygen consumption correlated well with ^{31}P-MRS-measured recovery rates of phosphocreatine after short duration exercise. Furthermore, both NIRS and ^{31}P-MRS measurements exhibited excellent repeatability and reproducibility. The level of agreement between NIRS and ^{31}P-MRS is similar to a previous study. Nagasawa et al. (27) made similar measurements in the forearm muscles of eight male participants. These authors reported a similar relationship between NIRS and ^{31}P-MRS recovery rates ($r = 0.92$). In contrast to the present study, the previous study did not utilize a correction for blood volume shifts. Nonetheless, the current study supports the findings reported by Nagasawa et al. (27). The recovery time constants in this study (31.5 ± 8.5 s for PCr and 31.5 ± 8.9 s for NIRS) are also similar those reported by previous studies using ^{31}P-MRS (10, 19, 39).

Previous studies have validated ^{31}P-MRS previously with more invasive muscle biopsy techniques. McCully et al. (21) compared PCr recovery rates and citrate synthase activities of ten healthy participants, reporting a significant correlation coefficient of ~0.71. Similarly, Larson-Meyer and colleagues (19) reported correlations between ^{31}P-MRS measured recovery rates (for both PCr and ADP) and citrate synthase activity levels of 0.48 – 0.64. Lanza et al. (18) compared PCr recovery rates (calculated Q_{max}) with in vitro high-resolution respirometry measurements of State 3 respiration. In this study, ^{31}P-MRS measure maximal oxidative capacity showed good agreement with State 3 respiration ($r = 0.66 – 0.72$). Using an animal model, Paganini et al. (28) found a similar

correlation between PCr recovery rates and citrate synthase activity ($r = 0.84$). NIRS recovery rates have not yet been compared to *in vitro* measurements of skeletal muscle oxidative capacity or mitochondrial function.

The direct comparisons between NIRS and ^{31}P-MRS in this study were made using a convenience sample of young healthy, college-aged individuals. This sample of individuals was chosen in order to achieve the highest quality of data possible. For this reason, we have also calculated signal-to-noise ratio (SNR) measurements for both NIRS and ^{31}P-MRS. Some potential factors that could influence the SNR of ^{31}P-MRS data include: leg positioning in comparison to the isocenter of the magnet, coil positioning and loading, shim quality, muscle composition (intramuscular fat and subcutaneous fat levels), and movement during in-magnet exercise protocols. There are several approaches to calculating SNR of magnetic resonance spectra. Some approaches account for differences in MR signal acquisition parameters (acquired flip angle, T_1 and T_2^* relaxation rate, and partial saturations) (30). The approach used in this study is a rather simple method for calculating *in vivo* SNR, that is easy to perform and similar to previous studies (1, 8, 40).

To our knowledge, this is the first study to provide a calculation of SNR for NIRS measurements of muscle oxygen consumption. The SNR of NIRS data are likely influenced by adipose tissue thickness, NIR-light intensity (gain settings on most commercially-available devices), source-detector distances, and possible movement artifact during testing. The sample of participants in this study include both males and females and had a modest range in adipose thickness. We found no evidence of a gender or adipose tissue thickness effect on the results of this study. Participants in this study

underwent familiarization of both NIRS and ^{31}P-MRS testing protocols prior to data collection to ensure the best possible data quality was collected. It is difficult to make direct comparisons of SNR between NIRS and ^{31}P-MRS, but using the approach describe here should allow for inter-laboratory comparisons of data quality for both methodologies. We suggest that future studies examine and report the SNR for both NIRS and ^{31}P-MRS, as this SNR likely contributes to the measurement variance of each methodology.

Because NIRS and ^{31}P-MRS measurements were in good agreement with one another, we attempted to quantify NIRS results (calculate a Q_{max} in mM O_2/s) based on the ^{31}P-MRS calculated Q_{max} (in mM ATP/s). According the electric analog model first presented by Meyer (24), a maximal rate of mitochondrial oxidative ATP synthesis could be calculated from the following equation:

$$Q_{max} = [PCr]_{rest} * k_{PCr} \qquad \text{(Equation 4.4)}$$

where $[PCr]_{rest}$ is the resting concentration of phosphocreatine and k_{PCr} is the rate constant for the recovery of PCr after exercise. Assuming a P:O_2 ratio of 6, this value can be converted to units of mM O_2/s. For the present study, the calculated Q_{max} (in mM O_2/s) from ^{31}P-MRS data was 0.193 ± 0.051. Since NIR-light is absorbed mainly by hemoglobin and myoglobin in skeletal muscle, the concentrations and relative saturations of these two molecules will influence the total oxygen content in the skeletal muscle. Calculations of total oxygen content were based on capillary densities, intravascular hemoglobin concentrations (in capillaries), and intramyocellular myoglobin concentrations (0.5 mM, van Beek-Harmsen (37)) reported recently by Davis and Barstow (7). Millimolar concentrations of hemoglobin and myoglobin were converted to

oxygen concentrations based on the respective molecular weights (~65000g/mole and 17000 g/mole for hemoglobin and myoglobin respectively), the oxygen carrying capacity (number of heme units = 4 for hemoglobin, and 1 for myoglobin), and relative saturations (79% and 91% for hemoglobin and myoglobin respectively). The maximal rate of mitochondrial oxygen consumption ($Qmax_{NIRS}$) was calculated from the following equation:

$$Qmax_{NIRS} = \text{Total } O_2 \text{ content} * k_{NIRS} \qquad \text{(Equation 4.5)}$$

For the present study, the calculated Q_{max} (in mM O_2/s) from NIRS data was 0.193 ± 0.052 and 0.191 ± 0.056 for Channel 1 and Channel 2 respectively. The average capillary density used in these calculations was 248 ± 71 capillaries/mm^2, which is inline with previous reported capillary densities in human skeletal muscle (3, 31, 35, 36). The quantification approach of NIRS data utilized several assumptions, which limits its generalizability. Individual variations in capillary densities, myoglobin concentrations, hematocrit, hemoglobin and myoglobin saturations, and P:O ratios are common in both humans and animals.

In conclusion, there was a good agreement between NIRS and ^{31}P-MRS indices of skeletal muscle oxidative capacity in young, healthy subjects. This supports the use of NIRS as a valid method for assessing skeletal muscle oxidative capacity. The absolute agreement in recovery rates between the NIRS and ^{31}P-MRS measurements suggest that direct comparisons between measurements of mitochondrial oxidative capacity can be made between the two types of measurements. Although this study reports good agreement between NIRS and ^{31}P-MRS, future studies are needed to determine the level

of agreement in clinical populations. Furthermore, both NIRS and ^{31}P-MRS measurements were very reproducible.

Acknowledgements

This study was funded in part by NIH HD039676. We would like to acknowledge Jared Brizendine and Michael Smith for their assistance with data collection during this study.

Author Contributions

T.E.R. and K.K.M. were responsible for conception and design of the research; T.E.R, W.M.S., and M.R. performed the experiments; T.E.R wrote the analysis routines and analyzed the data; T.E.R., W.M.S., M.R., and K.K.M. interpreted the results of the experiments; T.E.R. prepared the figures; T.E.R. drafted the manuscript; T.E.R., W.M.S, M.R., and K.K.M. edited and revised the manuscript; T.E.R., W.M.S, M.R., and K.K.M. approved the final version of the manuscript.

Conflict of interest statement

The authors report no conflicts of interest

References

1. Boska MD, Hubesch B, Meyerhoff DJ, Twieg DB, Karczmar GS, Matson GB, and Weiner MW. Comparison of 31P MRS and 1H MRI at 1.5 and 2.0 T. *Magn Reson Med* 13: 228-238, 1990.

2. Brizendine JT, Ryan TE, Larson RD, and McCully KK. Skeletal Muscle Metabolism in Endurance Athletes with Near-Infrared Spectroscopy. *Med Sci Sports Exerc* 2012.

3. Celsing F, Ekblom B, Sylven C, Everett J, and Astrand PO. Effects of chronic iron deficiency anaemia on myoglobin content, enzyme activity, and capillary density in the human skeletal muscle. *Acta Med Scand* 223: 451-457, 1988.

4. Chance B, Im J, Nioka S, and Kushmerick M. Skeletal muscle energetics with PNMR: personal views and historic perspectives. *NMR In Biomedicine* 19: 904-926, 2006.

5. Chance B, and Williams GR. Respiratory enzymes in oxidative phosphorylation. IV. The respiratory chain. *The Journal of biological chemistry* 217: 429-438, 1955.

6. Conley KE, Jubrias SA, and Esselman PC. Oxidative capacity and ageing in human muscle. *J Physiol-London* 526: 203-210, 2000.

7. Davis ML, and Barstow TJ. Estimated contribution of hemoglobin and myoglobin to near infrared spectroscopy. *Respir Physiol Neurobiol* 186: 180-187, 2013.

8. Drost DJ, Riddle WR, Clarke GD, and Group AMT. Proton magnetic resonance spectroscopy in the brain: report of AAPM MR Task Group #9. *Med Phys* 29: 2177-2197, 2002.

9. Erickson ML, Ryan TE, Young HJ, and McCully KK. Near-infrared assessments of skeletal muscle oxidative capacity in persons with spinal cord injury. *European Journal Of Applied Physiology* 2012.

10. Forbes SC, Paganini AT, Slade JM, Towse TF, and Meyer RA. Phosphocreatine recovery kinetics following low- and high-intensity exercise in human triceps surae and rat posterior hindlimb muscles. *American Journal Of Physiology Regulatory, Integrative And Comparative Physiology* 296: R161-R170, 2009.

11. Gnaiger E. Capacity of oxidative phosphorylation in human skeletal muscle: new perspectives of mitochondrial physiology. *Int J Biochem Cell Biol* 41: 1837-1845, 2009.

12. Gollnick PD, Armstrong RB, Saltin B, Saubert CWt, Sembrowich WL, and Shepherd RE. Effect of training on enzyme activity and fiber composition of human skeletal muscle. *J Appl Physiol* 34: 107-111, 1973.

13. Holloszy JO. Biochemical adaptations in muscle. Effects of exercise on mitochondrial oxygen uptake and respiratory enzyme activity in skeletal muscle. *J Biol Chem* 242: 2278-2282, 1967.

14. Holloszy JO, Oscai LB, Don IJ, and Mole PA. Mitochondrial citric acid cycle and related enzymes: adaptive response to exercise. *Biochem Biophys Res Commun* 40: 1368-1373, 1970.

15. Hopkins WG. Reliability from consecutive pairs of trials. In: A nice view of statistics of statics. http://sportsci.org/resource/stats/xrely.xls. [Jan 10, 2011, 2011].

16. Joseph AM, Joanisse DR, Baillot RG, and Hood DA. Mitochondrial dysregulation in the pathogenesis of diabetes: potential for mitochondrial biogenesis-mediated interventions. *Exp Diabetes Res* 2012: 642038, 2012.

17. Kent-Braun JA, Sharma KR, Miller RG, and Weiner MW. Postexercise phosphocreatine resynthesis is slowed in multiple sclerosis. *Muscle Nerve* 17: 835-841, 1994.

18. Lanza IR, Bhagra S, Nair KS, and Port JD. Measurement of human skeletal muscle oxidative capacity by 31P-MR spectroscopy: A cross-validation with in vitro measurements. *J Magn Reson Imaging* n/a-n/a, 2011.

19. Larson-Meyer DE, Newcomer BR, Hunter GR, Joanisse DR, Weinsier RL, and Bamman MM. Relation between in vivo and in vitro measurements of skeletal muscle oxidative metabolism. *Muscle Nerve* 24: 1665-1676, 2001.

20. Lodi R, Taylor DJ, and Schapira AH. Mitochondrial dysfunction in friedreich's ataxia. *Biol Signals Recept* 10: 263-270, 2001.

21. McCully KK, Fielding RA, Evans WJ, Leigh JS, Jr., and Posner JD. Relationships between in vivo and in vitro measurements of metabolism in young and old human calf muscles. *Journal Of Applied Physiology (Bethesda, Md: 1985)* 75: 813-819, 1993.

22. McCully KK, Forciea MA, Hack LM, Donlon E, Wheatley RW, Oatis CA, Goldberg T, and Chance B. Muscle metabolism in older subjects using 31P magnetic resonance spectroscopy. *Can J Physiol Pharm* 69: 576-580, 1991.

23. McCully KK, Mulcahy TK, Ryan TE, and Zhao Q. Skeletal muscle metabolism in individuals with spinal cord injury. *Journal of Applied Physiology* 111: 143-148, 2011.

24. Meyer RA. A linear model of muscle respiration explains monoexponential phosphocreatine changes. *American Journal of Physiology - Cell Physiology* 254: C548-C553, 1988.

25. Mitchell P. Coupling of phosphorylation to electron and hydrogen transfer by a chemi-osmotic type of mechanism. *Nature* 191: 144-148, 1961.

26. Motobe M, Murase N, Osada T, Homma T, Ueda C, Nagasawa T, Kitahara A, Ichimura S, Kurosawa Y, Katsumura T, Hoshika A, and Hamaoka T. Noninvasive monitoring of deterioration in skeletal muscle function with forearm cast immobilization and the prevention of deterioration. *Dyn Med* 3: 2, 2004.

27. Nagasawa T, Hamaoka T, Sako T, Murakami M, Kime R, Homma T, Ueda C, Ichimura S, and Katsumura T. A practical indicator of muscle oxidative capacity determined by recovery of muscle O 2 consumption using NIR spectroscopy. *European Journal of Sport Science* 3: 1-10, 2003.

28. Paganini AT, Foley JM, and Meyer RA. Linear dependence of muscle phosphocreatine kinetics on oxidative capacity. *Am J Physiol-Cell Ph* 272: C501-C510, 1997.

29. Petersen KF, Dufour S, Befroy D, Garcia R, and Shulman GI. Impaired mitochondrial activity in the insulin-resistant offspring of patients with type 2 diabetes. *N Engl J Med* 350: 664-671, 2004.

30. Qiao H, Zhang X, Zhu XH, Du F, and Chen W. In vivo 31P MRS of human brain at high/ultrahigh fields: a quantitative comparison of NMR detection sensitivity and spectral resolution between 4 T and 7 T. *Magn Reson Imaging* 24: 1281-1286, 2006.

31. Richardson RS, Poole DC, Knight DR, and Wagner PD. Red blood cell transit time in man: theoretical effects of capillary density. *Adv Exp Med Biol* 361: 521-532, 1994.

32. Ryan TE, Brizendine JT, and McCully KK. A comparison of exercise type and intensity on the noninvasive assessment of skeletal muscle mitochondrial function using near-infrared spectroscopy. *J Appl Physiol* 114: 230-237, 2013.

33. Ryan TE, Erickson ML, Brizendine JT, Young HJ, and McCully KK. Noninvasive evaluation of skeletal muscle mitochondrial capacity with near-infrared spectroscopy: correcting for blood volume changes. *Journal of Applied Physiology* 113: 175-183, 2012.

34. Ryan TE, Southern WM, Reynolds MA, and McCully KK. Activity-induced changes in skeletal muscle metabolism with optical spectroscopy. *Medicine & Science in Sports & Exercise* 2013.

35. Terrados N, Jansson E, Sylven C, and Kaijser L. Is hypoxia a stimulus for synthesis of oxidative enzymes and myoglobin? *J Appl Physiol* 68: 2369-2372, 1990.

36. Terrados N, Melichna J, Sylven C, and Jansson E. Decrease in skeletal muscle myoglobin with intensive training in man. *Acta Physiol Scand* 128: 651-652, 1986.

37. van Beek-Harmsen BJ, Bekedam MA, Feenstra HM, Visser FC, and van der Laarse WJ. Determination of myoglobin concentration and oxidative capacity in cryostat sections of human and rat skeletal muscle fibres and rat cardiomyocytes. *Histochemistry and cell biology* 121: 335-342, 2004.

38. Vorgerd M, Schols L, Hardt C, Ristow M, Epplen JT, and Zange J. Mitochondrial impairment of human muscle in Friedreich ataxia in vivo. *Neuromuscul Disord* 10: 430-435, 2000.

39. Walter G, Vandenborne K, McCully KK, and Leigh JS. Noninvasive measurement of phosphocreatine recovery kinetics in single human muscles. *Am J Physiol-Cell Ph* 41: C525-C534, 1997.

40. Wylezinska M, Cobbold JF, Fitzpatrick J, McPhail MJ, Crossey MM, Thomas HC, Hajnal JV, Vennart W, Cox IJ, and Taylor-Robinson SD. A comparison of single-voxel clinical in vivo hepatic 31P MR spectra acquired at 1.5 and 3.0 Tesla in health and diseased states. *NMR Biomed* 24: 231-237, 2011.

Table 4.1. Physical characteristics of the participants.

	Height *(cm)*	**Weight** *(kg)*	**BMI** *(kg/m^2)*	**Age** *(yr)*	**ATT** *(mm)*	**Optode Distance (mm)** *Ch 1*	*Ch2*
Males (*n* = 10)	179.1 ± 6.4	79.9 ± 12.2	24.8 ± 3.1	23.0 ± 3.2	6.1 ± 1.6	-	-
Females (*n* = 6)	168.1 ± 9.6	68.1 ± 11.6	24.0 ± 1.7	21.6 ± 2.6	9.1 ± 3.4	-	-
Total (*n* = 16)	174.9 ± 9.2	75.5 ± 13.0	24.5 ± 2.6	22.5 ± 3.0	7.2 ± 2.8	30/35 (*n* = 11/6)	40/45 (*n* = 11/6)

Note: Data presented as means ± SD. ATT = adipose tissue thickness over site of NIRS optode. NIRS optode distances used and their corresponding frequency of use are shown for informational reasons. Statistical comparisons between genders were not performed.

Table 4.2. Resting and end-exercise [PCr] and pH.

	Resting		**End Exercise**	
Variable	*[PCr]*	*pH*	*[PCr]*	*pH (minimum)*
All Participants	34.25 ± 2.86	7.05 ± 0.03	25.89 ± 2.96	7.01 ± 0.07 (6.98 ± 0.06)

Abbreviations: PCr, phosphocreatine. End-exercise pH was calculated from the first phosphorus spectra during the recovery measurements. The minimum pH is the lowest pH recorded during the recovery measurements.
Values presented as mean ± SD.

Table 4.3. NIRS and ^{31}P-MRS metabolic parameters

	Trial 1	Trial 2	CV (%) [Range]	ICC	Pearson's *r*	*P* (paired t-test)
NIRS Parameters						
Channel 1						
End-exercise mVO_2 (%/s)	5.1 ± 1.2	5.4 ± 2.0	9.8 [0.2 – 57.4]	0.85	0.827	0.311
Time Constant (s)	30.5 ± 9.5	32.2 ± 8.6	8.1 [0.2 – 15.7]	0.93	0.936	0.599
k_{NIRS} (s^{-1})	0.0353 ± 0.0091	0.0329 ± 0.0078	8.1 [0.2 – 15.7]	0.93	0.838	0.513
Q_{max} (mM O_2/s)	0.200 ± 0.055	0.186 ± 0.046	8.1 [0.2 – 15.7]	0.93	0.899	0.039
Channel 2						
End-exercise mVO_2 (%/s)	5.2 ± 1.8	5.5 ± 2.0	8.9 [0.2 – 52.1]	0.83	0.813	0.289
Time Constant (s)	31.2 ± 9.7	33.0 ± 9.6	6.9 [0.2 -15.7]	0.95	0.925	0.720
k_{NIRS} (s^{-1})	0.0347 ± 0.0095	0.0326 ± 0.0085	6.9 [0.2 -15.7]	0.95	0.936	0.164
Q_{max} (mM O_2/s)	0.197 ± 0.059	0.186 ± 0.054	6.9 [0.2 – 15.7]	0.95	0.929	0.044
^{31}P-MRS Parameters						
End-exercise PCr (mM)	25.73 ± 3.00	26.05 ± 3.01	3.8 [0.4 – 12.9]	0.87	0.848	0.463
End-exercise pH	7.00 ± 0.08	7.02 ± 0.06	0.3 [0.0 – 1.1]	0.86	0.896	0.150
Time Constant (s)	31.3 ± 8.2	31.8 ± 9.4	7.6 [1.3 – 19.7]	0.90	0.896	0.639
k_{PCr} (s^{-1})	0.0338 ± 0.0078	0.0337 ± 0.0086	7.6 [1.3 – 19.7]	0.90	0.862	0.946
Q_{max} (mM ATP/s)	1.16 ± 0.28	1.16 ± 0.32	7.6 [2.3 – 19.7]	0.89	0.883	0.999
Q_{max} (mm O_2/s)	0.193 ± 0.047	0.193 ± 0.54	7.6 [2.3 – 19.7]	0.89	0.883	0.998

Data are presented as mean ± SD. Abbreviations: CV = coefficient of variation; ICC = intraclass correlation coefficient; mVO_2 = muscle oxygen consumption; k_{NIRS} = rate constant for the recovery or mVO_2; k_{PCr} = rate constant for the recovery of PCr; Q_{max} = maximal rate of oxygen consumption (in mM O_2/s) or maximal rate of ATP synthesis (in mM ATP/s); PCr = phosphocreatine.

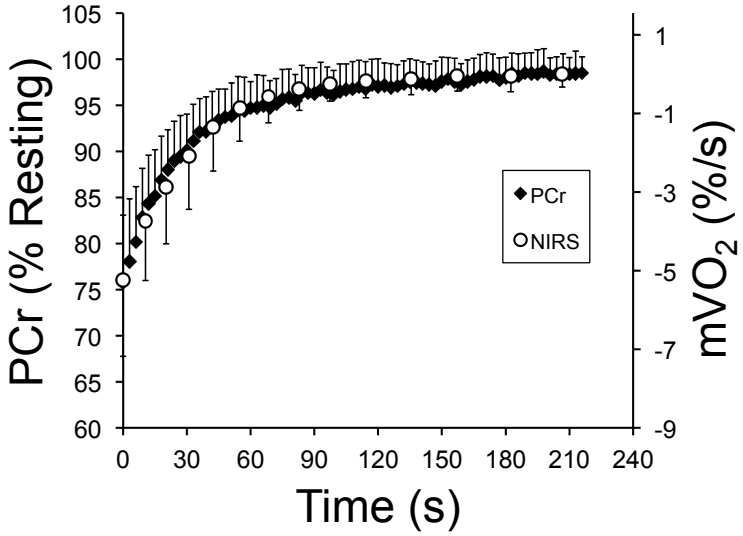

Figure 4.1. Recovery of phosphocreatine (PCr) and muscle oxygen consumption (mVO_2) after short duration plantarflexion exercise. Data are presented as the mean of all participants and all trials, with the error bars representing the SD.

^{31}P-MRS

A

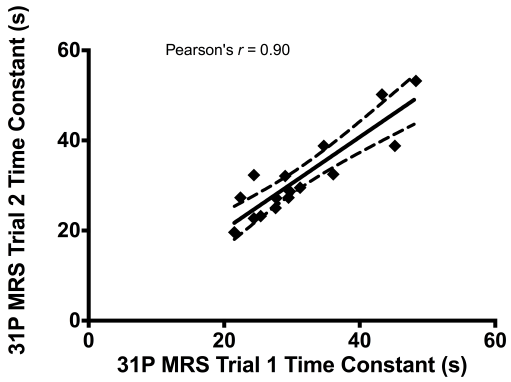

B

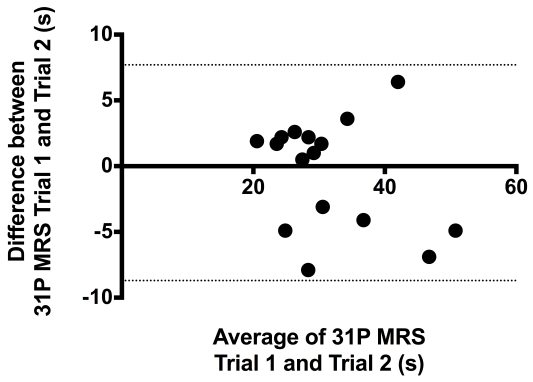

NIRS Channel 1

C

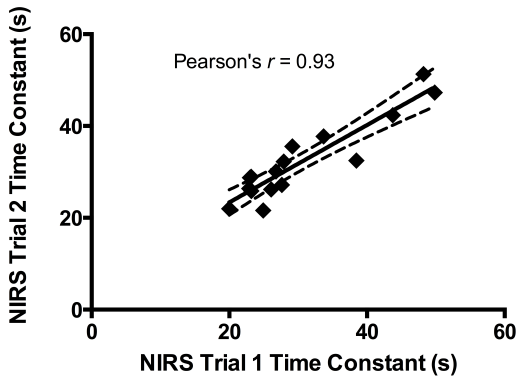

D

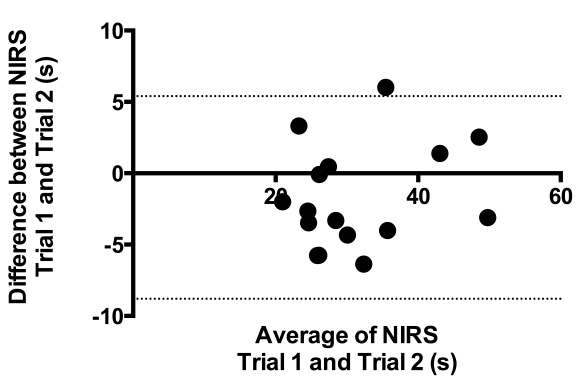

NIRS Channel 2

E

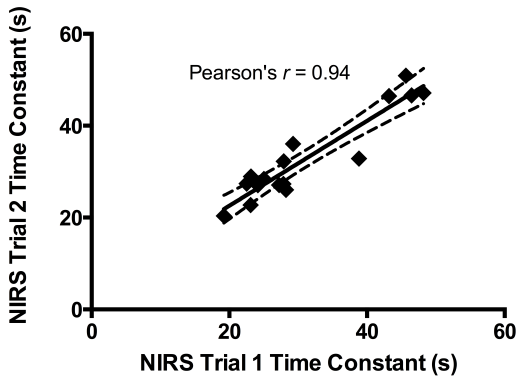

F

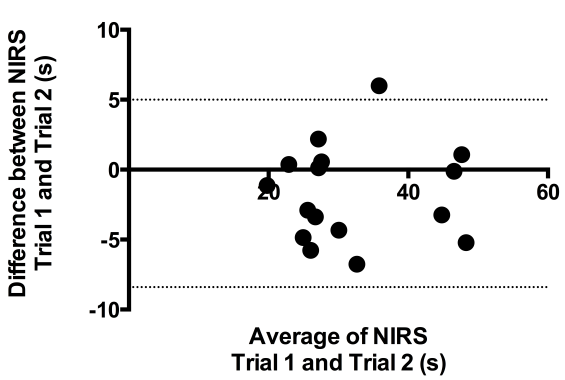

Figure 4.2. Repeatability and reproducibility of ^{31}P-MRS and NIRS data. Linear regression comparisons between trials are shown for ^{31}P-MRS (A), NIRS Channel 1 (C), and NIRS Channel 2 (E). For subplots A, C, and E, the dotted lines represent the 95% confidence intervals for the regression equation. Corresponding Bland-Altman plots are shown for ^{31}P-MRS (B), NIRS Channel 1 (D), and NIRS Channel 2 (F). For Bland-Altman plots, dotted lines represent the 95% limits of agreement.

^{31}P-MRS vs. NIRS Channel 1

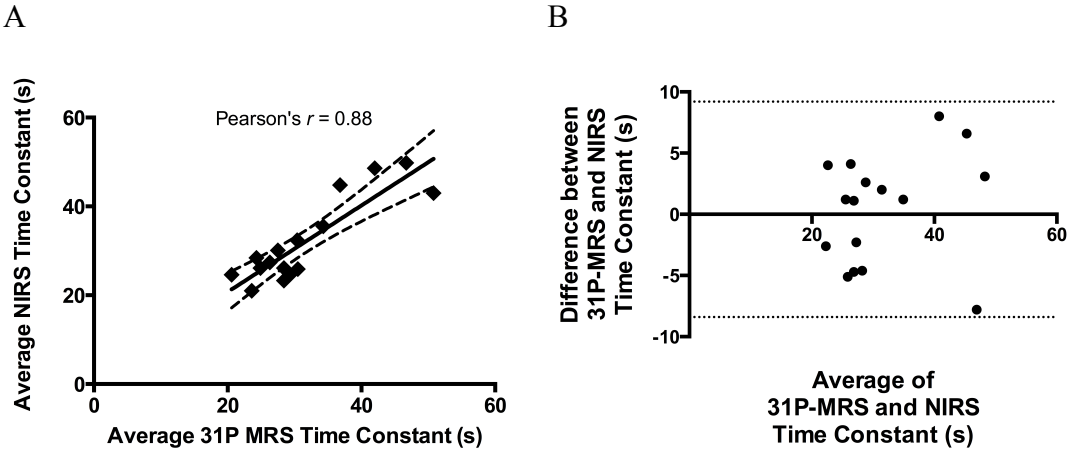

^{31}P-MRS vs. NIRS Channel 2

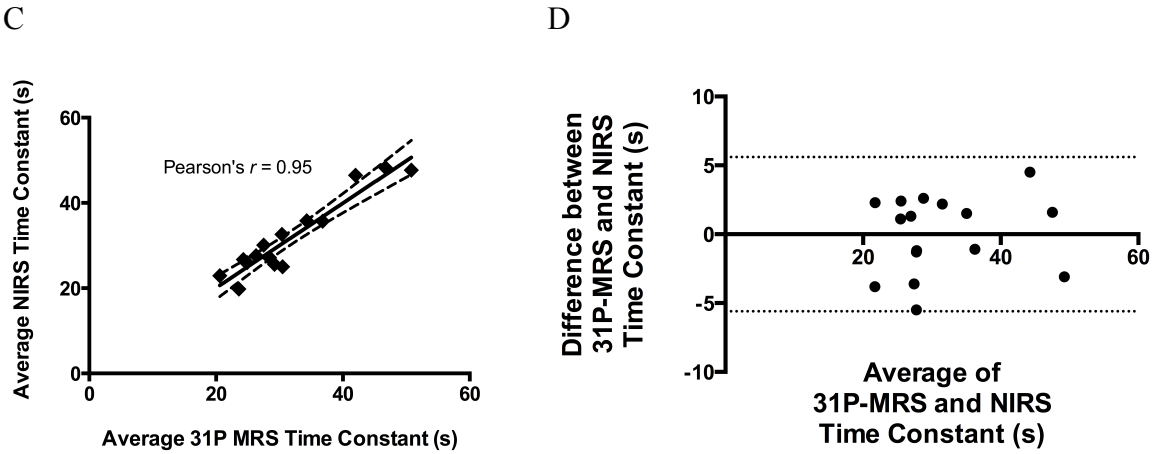

Figure 4.3. Comparison between ^{31}P-MRS and NIRS data. All comparisons were made by averaging the time constants for both trials. Linear regression comparisons between ^{31}P-MRS and NIRS Channel 1 (A) and NIRS Channel 2 (C), where dotted lines represent the 95% confidence intervals for the regression equation. Corresponding Bland-Altman plots for comparisons between ^{31}P-MRS and NIRS Channel 1 (B) and NIRS Channel 2 (D) are also shown, with the dotted lines indicating the 95% limits of agreement.

A

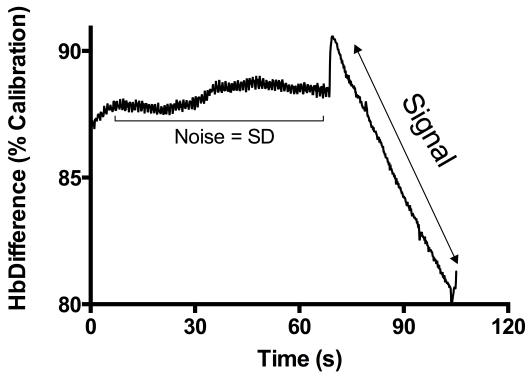

B

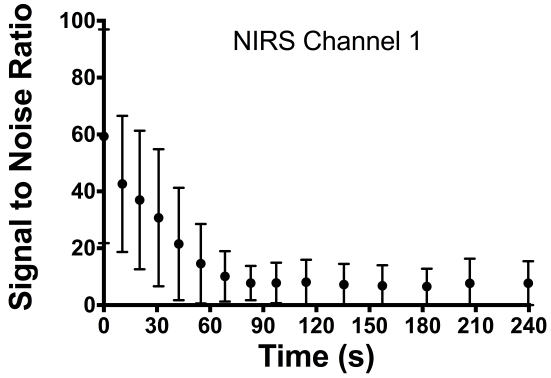

C

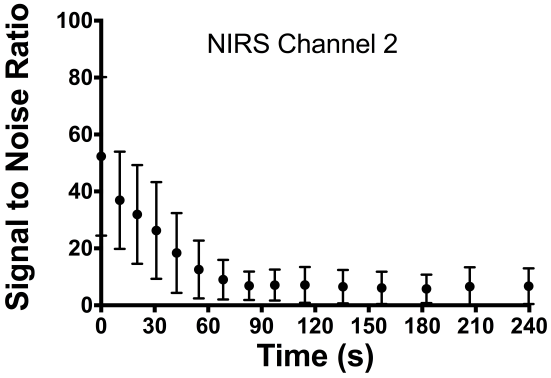

Figure 4.4: Signal-to-noise analysis of NIRS data. A sample NIRS signal showing how the signal-to-noise ratio (SNR) was calculated is shown in panel A. SNR ratios for each post-exercise arterial occlusion are shown for Channel 1 (B) and Channel 2 (C). Data in panels B and C are the average of all participant and all trials, with error bars representing SD.

A

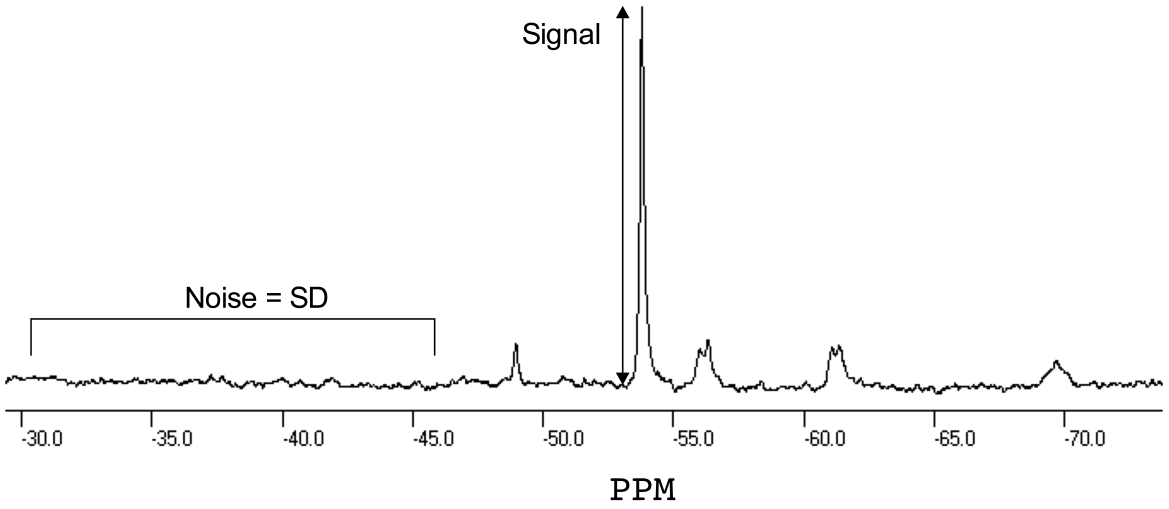

B

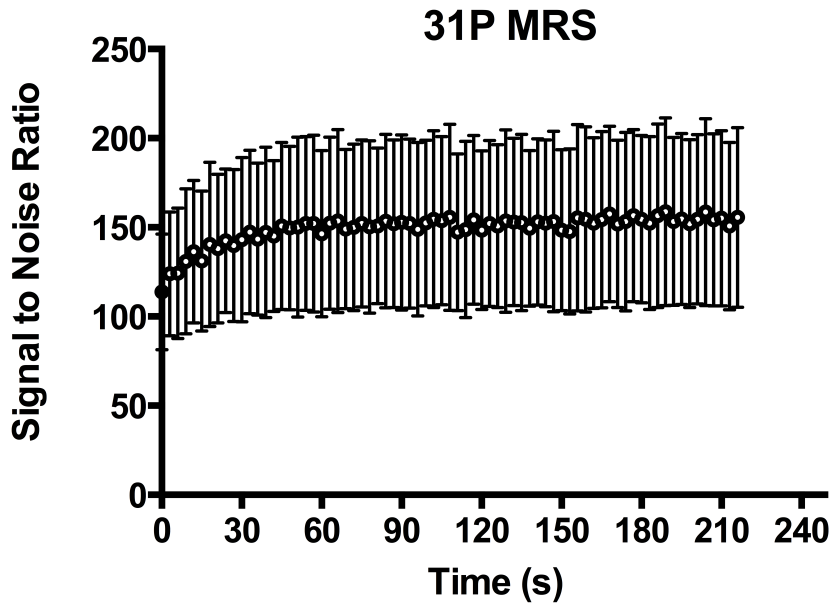

Figure 4.5. Signal-to-noise analysis of ^{31}P-MRS data. Panel A shows a single phosphorus spectra; after apodization, zero filling, and Fourier transformation. The average signal-to-noise ratio (SNR) during the post-exercise recovery for all participants and all trials is shown panel B, where error bars represent the SD.

CHAPTER 5

SUMMARY AND CONCLUSIONS

The primary purpose of these studies was to validate a novel *in vivo* approach to measuring skeletal muscle mitochondrial function using near infrared spectroscopy (NIRS). These studies represent important steps in the development of this methodology, and provide some essential validity to support near infrared spectroscopy as an important, new technique that may be useful both in research and clinical settings.

The findings from these studies suggest that NIRS is capable of accurately and reliably measuring changes in skeletal muscle mitochondrial function. In the first study, endurance exercise training was used to induce a change in mitochondrial function of the forearm muscles. NIRS was successfully able to track the changes in mitochondrial function, as indicated by increase in the NIRS recovery rate constant. The technique could also be useful in determining the effectiveness of other interventions, such as pharmacological or nutritional interventions. The second study made direct comparisons between NIRS measurements of mitochondrial function and phosphorus magnetic resonance spectroscopy (^{31}P-MRS) measurements of mitochondrial function. ^{31}P-MRS is generally considered to be the *gold standard* method for assessing *in vivo* mitochondrial function, and has been used for a number or years (3). The strong agreement between NIRS and ^{31}P-MRS suggest that NIRS is a valid method for evaluating mitochondrial function, and that NIRS recovery rates can be directly compared to ^{31}P-MRS.

The NIRS measurement method should have significant impact in the scientific community. More invasive techniques used to measure mitochondrial function require

muscle biopsies: a surgical removal of a small tissue sample. The invasiveness of these approaches limits their use in human participants. Furthermore, there can be significant cost associated with the reagents and other non-reusable supplies required for these biochemical techniques. Magnetic resonance spectroscopy, while not invasive, is still a very expensive technique. Multi-nuclear magnets are very expensive (~$2,000,000) and require additional costs for coils, MRI technicians, MRI engineers, and other maintenance, etc. In addition, there is usually an hourly cost associated with the use of the MRI. In contrast, NIRS devices are relatively inexpensive (~$10,000 - $50,000). In addition to the NIRS devices, the cost of other equipment (air compressor, cuff inflator, computer analysis software) is also relatively low (~$5,000). NIRS is a more affordable, portable, and available technology for measuring mitochondrial function.

It has been know for several years that a number of different molecules, known as chromophores, can absorb NIR light. In regards to skeletal muscle applications, intravascular hemoglobin, intramyocellular myoglobin, cytochromes in the mitochondrial electron transport chain, and melanin from skin overlying the muscle tissue can absorb NIR light (6-8, 10, 15-18). The absorption spectra of these chromophores in the NIR region have subtle differences. Both melanin and cytochrome have greater absorption at lower wavelengths (300 – 500 nm), while hemoglobin and myoglobin have greater absorption at higher wavelengths (600 – 900 nm). The relative contributions of hemoglobin and myoglobin to the NIRS signal are controversial. Some studies suggest that hemoglobin is the main contributor (10, 15); while others, Davis and Barstow (4) and Marcinek et al. (11) have suggested that myoglobin is the main absorber of NIR light in skeletal muscle. Currently available NIRS devices make the assumption that hemoglobin

and myoglobin have identical absorption spectra for the NIR light wavelengths, and therefore cannot distinguish between the two. Since myoglobin and hemoglobin have different oxygen binding characteristics (i.e. number of O_2 binding sites, and binding affinities) it is possible that their relative contributions to the NIRS signal could influence the measurements used in these studies. Future NIRS devices may be capable of distinguishing between myoglobin and hemoglobin, and subsequent studies could be of interest.

Both studies presented here utilized a convenience sample of young, healthy, college-aged adults. During the design of both experiments, we decided to use this type of sample to produce the best possible data quality for both NIRS and ^{31}P-MRS. All individuals were free of disease and relatively thin. Skin and fat thickness overlying the muscle can influence both NIRS and ^{31}P-MRS approaches in these studies since both techniques utilized surface-mounted probes (NIRS optode and MRS surface coil). The individuals in these studies were all relatively lean, which the adipose tissue thickness ranging from 2.8 – 9.8 mm in the forearm and 3.2 – 13.8 mm in the calf. Currently available NIRS devices may have a limited ability to study overweight or obese populations due to their relatively shallow sampling depth (less than 3 cm for most devices). Both studies presented here used an Oxymon MkIII (Artinis Medical Systems, The Netherlands). This NIRS device uses fiber optic cables to transmit NIR light from the unit to the probe attached to the tissue of interest. This device has some advantages over wireless NIRS devices including: an ability to alter the source-detector distance, and some control of NIR light gain setting. Adjusting the NIR light gain settings allows the user to increase or decrease the light intensity (given manufacturer presets) in order to

optimize the NIRS signal for the best quality data collection. It is possible that higher end NIRS devices (time or frequency domain NIRS devices) could perform even better than device used in these studies, but future studies are needed. During the data analysis phase of study 2, we developed approaches to measure the signal quality of NIRS and ^{31}P-MRS, by calculating signal-to-noise ratios (SNR). The approach to assessing data quality should allow for between lab comparisons of results. It is possible that data collected from clinical populations such as cardiovascular disease, heart failure, diabetes, multiple sclerosis, and obese individuals may results in lower SNR's. Decreased SNR could influence the variance of NIRS measurements. Future studies are necessary to determine the SNR of NIRS data in clinical populations, as well as the level of agreement between NIRS and ^{31}P-MRS.

While NIRS can be used to measure the oxidative capacity of skeletal muscle mitochondria, the mechanisms behind alterations cannot be determined from NIRS. For example, the increased NIRS rate constant reported in study 1, in response to forearm endurance exercise training, could be a result of improved mitochondrial enzyme capacity (i.e. ATP synthase activity) or an increase in the number of mitochondria (i.e. mitochondrial density) within the NIRS measured tissue. NIRS cannot distinguish between changes in mitochondrial density or enzyme activity. It is likely that endurance exercise training produced both improve enzyme activity and increased mitochondrial density, this is a limitation of NIRS, as well as ^{31}P-MRS. These *in vivo* approaches provide information about the 'function' of the intact organelle, in its native environment with intact circulatory and regulatory systems. In vitro approaches can allow researchers to further examine the mechanisms behind increases or decreases in mitochondrial

function. For example, high resolution respirometry can allows the researcher to examine the function of each multi-polypeptide complex of the electron transport chain, and determine the specific mechanisms for the observed results.

Another potential limitation of NIRS is the quantification of data. In the current studies, NIRS data were analyzed and expressed as a percentage of change in the NIRS signal per unit time. For instance, muscle oxygen consumption during arterial occlusions was expressed as a percentage change in the NIRS signal (scaled to the maximal physiological range). Expressing NIRS oxygen consumption in absolute terms (millimolar oxygen per unit time) should allow more accurate comparisons between individuals and NIRS devices. However, the current NIRS devices are unable to accurately quantify changes in NIRS signals, even more advanced devices capable of measuring the NIR light pathlength and other important absorption/scattering characteristics (9). In the second study, we attempted to quantify NIRS recovery rates, and calculate a maximal rate of oxygen consumption from the NIRS rate constant. We were able to calculate maximal rates of oxygen consumption that had reasonable agreement with those calculated more directly from ^{31}P-MRS data. Using assumptions about the concentrations of hemoglobin and myoglobin (taken from published data), the relative saturations of hemoglobin and myoglobin, and the mitochondrial adenosine triphosphate:oxygen ratio (ATP:O ratio) we were able to calculate a total tissue oxygen content, which when multiplied by the NIRS rate constant gives the maximal rate of oxygen consumption. While these quantifications are promising, the assumptions made are unlikely to be valid for all individuals or all populations, and thus limits the generalizability of this quantification approach.

One interesting component of these studies, which was not emphasized previously, is the data analysis for magnetic resonance spectroscopy and near infrared spectroscopy experiments. Both techniques presented here produce large, complex sets of data, which cannot be analyzed using standard spreadsheet software's (i.e. Microsoft Excel). For example, each phosphorus magnetic resonance data set (exercise/recovery protocol) contains 100 spectra, each containing 8192 data points (100 x 8192 array), both real and imaginary. Similarly, a typical NIRS test contains an array of 10 x ~20,000 data points, since the NIRS device outputs several signals and channels. Considering that study 1 consisted of approximately 180 NIRS tests, semi-automated custom written analysis software is a necessity. Data collected in these studies were analyzed using custom-written routines in Matlab (Mathworks, Natick, MA). Without these routines, data analysis for the current studies would have taken considerably longer. A portion of the NIRS data analysis utilized a patent-pending correction algorithm for small shifts in blood volume (Inventors: Terence Ryan and Kevin McCully). This correct improves the accuracy of skeletal muscle oxygen consumption measurements by removing small artifacts in the NIRS signals due to blood volume shifts. The use of the correct seems to be vital for continuous wave NIRS devices, like the one used in these studies. Future studies will need to assess blood volume shifts in other NIRS devices (time- and frequency domain).

In summary, the findings of these studies provide essential validation for a novel in vivo approach for measuring skeletal muscle oxidative capacity. In combination with previous studies, NIRS measurements of skeletal muscle oxidative capacity have been shown to be reproducible (2, 14), independent of exercise type and intensity (13); can

detect the expected differences in mitochondrial function between sedentary individuals and endurance trained cyclists (1); as well as detect the differences between sedentary individuals and motor complete spinal cord injuries (5). These studies suggest that NIRS can also be used to track changes in response to exercise training and detraining; and shows good agreement with ^{31}P-MRS, consistent with previous studies (12). NIRS is an exciting new technology that certainly hold promise for the future. With the relatively low cost of NIRS devices and ease of use this technique should be highly useful to both researchers and clinicians.

References

1. Brizendine JT, Ryan TE, Larson RD, and McCully KK. Skeletal Muscle Metabolism in Endurance Athletes with Near-Infrared Spectroscopy. *Med Sci Sports Exerc* 2012.

2. Buchheit M, Ufland P, Haydar B, Laursen PB, and Ahmaidi S. Reproducibility and sensitivity of muscle reoxygenation and oxygen uptake recovery kinetics following running exercise in the field. *Clin Physiol Funct Imaging* 31: 337-346, 2011.

3. Chance B, Im J, Nioka S, and Kushmerick M. Skeletal muscle energetics with PNMR: personal views and historic perspectives. *NMR In Biomedicine* 19: 904-926, 2006.

4. Davis ML, and Barstow TJ. Estimated contribution of hemoglobin and myoglobin to near infrared spectroscopy. *Respir Physiol Neurobiol* 186: 180-187, 2013.

5. Erickson ML, Ryan TE, Young HJ, and McCully KK. Near-infrared assessments of skeletal muscle oxidative capacity in persons with spinal cord injury. *European Journal Of Applied Physiology* 2012.

6. Ferrari M, Wilson DA, Hanley DF, Hartmann JF, Rogers MC, and Traystman RJ. Noninvasive determination of hemoglobin saturation in dogs by derivative near-infrared spectroscopy. *Am J Physiol* 256: H1493-1499, 1989.

7. Ferrari M, Wilson DA, Hanley DF, Hartmann JF, and Traystman RJ. Determination of cerebral venous hemoglobin saturation by derivative near infrared spectroscopy. *Adv Exp Med Biol* 248: 47-53, 1989.

8. Hampson NB, and Piantadosi CA. Near infrared monitoring of human skeletal muscle oxygenation during forearm ischemia. *J Appl Physiol* 64: 2449-2457, 1988.

9. Koga S, Poole DC, Fukuoka Y, Ferreira LF, Kondo N, Ohmae E, and Barstow TJ. Methodological validation of the dynamic heterogeneity of muscle deoxygenation within the quadriceps during cycle exercise. *American Journal Of Physiology Regulatory, Integrative And Comparative Physiology* 301: R534-541, 2011.

10. Mancini DM, Bolinger L, Li H, Kendrick K, Chance B, and Wilson JR. Validation of near-Infrared Spectroscopy in Humans. *Journal of Applied Physiology* 77: 2740-2747, 1994.

11. Marcinek DJ, Amara CE, Matz K, Conley KE, and Schenkman KA. Wavelength shift analysis: a simple method to determine the contribution of hemoglobin and myoglobin to in vivo optical spectra. *Appl Spectrosc* 61: 665-669, 2007.

12. Nagasawa T, Hamaoka T, Sako T, Murakami M, Kime R, Homma T, Ueda C, Ichimura S, and Katsumura T. A practical indicator of muscle oxidative capacity determined by recovery of muscle O 2 consumption using NIR spectroscopy. *European Journal of Sport Science* 3: 1-10, 2003.

13. Ryan TE, Brizendine JT, and McCully KK. A comparison of exercise type and intensity on the noninvasive assessment of skeletal muscle mitochondrial function using near-infrared spectroscopy. *J Appl Physiol* 114: 230-237, 2013.

14. Ryan TE, Erickson ML, Brizendine JT, Young HJ, and McCully KK. Noninvasive evaluation of skeletal muscle mitochondrial capacity with near-infrared spectroscopy: correcting for blood volume changes. *Journal of Applied Physiology* 113: 175-183, 2012.

15. Seiyama A, Hazeki O, and Tamura M. Noninvasive quantitative analysis of blood oxygenation in rat skeletal muscle. *Journal of biochemistry* 103: 419-424, 1988.

16. Tamura M, Hazeki O, Nioka S, Chance B, and Smith DS. The simultaneous measurements of tissue oxygen concentration and energy state by near-infrared and nuclear magnetic resonance spectroscopy. *Adv Exp Med Biol* 222: 359-363, 1988.

17. Wolf M, Ferrari M, and Quaresima V. Progress of near-infrared spectroscopy and topography for brain and muscle clinical applications. *Journal Of Biomedical Optics* 12: 062104, 2007.

18. Wray S, Cope M, Delpy DT, Wyatt JS, and Reynolds EO. Characterization of the near infrared absorption spectra of cytochrome aa3 and haemoglobin for the non-invasive monitoring of cerebral oxygenation. *Biochim Biophys Acta* 933: 184-192, 1988.